The peripheral preview effect with faces: Combined EEG and eye-tracking suggests multiple stages of trans-saccadic predictive and non-predictive processing

Christoph Huber-Huber [a,*], Antimo Buonocore [b,c], Olaf Dimigen [d], Clayton Hickey [a], David Melcher [a]

[a] Center for Mind/Brain Sciences (CIMeC), University of Trento, Corso Bettini 31, Rovereto, TN, 38068, Italy
[b] Werner Reichardt Centre for Integrative Neuroscience, Tuebingen University, Otfried-Müller-Straße 25, Tuebingen, 72076, Germany
[c] Hertie Institute for Clinical Brain Research, Tuebingen University, Tuebingen, 72076, Germany
[d] Department of Psychology, Humboldt-Universität zu Berlin, Unter Den Linden 6, 10099, Berlin, Germany

ARTICLE INFO

ABSTRACT

The world appears stable despite saccadic eye-movements. One possible explanation for this phenomenon is that the visual system predicts upcoming input across saccadic eye-movements based on peripheral preview of the saccadic target. We tested this idea using concurrent electroencephalography (EEG) and eye-tracking. Participants made cued saccades to peripheral upright or inverted face stimuli that changed orientation (invalid preview) or maintained orientation (valid preview) while the saccade was completed. Experiment 1 demonstrated better discrimination performance and a reduced fixation-locked N170 component (fN170) with valid than with invalid preview, demonstrating integration of pre- and post-saccadic information. Moreover, the early fixation-related potentials (FRP) showed a preview face inversion effect suggesting that some pre-saccadic input was represented in the brain until around 170 ms post fixation-onset. Experiment 2 replicated Experiment 1 and manipulated the proportion of valid and invalid trials to test whether the preview effect reflects context-based prediction across trials. A whole-scalp *Bayes factor* analysis showed that this manipulation did not alter the fN170 preview effect but did influence the face inversion effect before the saccade. The pre-saccadic inversion effect declined earlier in the mostly invalid block than in the mostly valid block, which is consistent with the notion of pre-saccadic expectations. In addition, in both studies, we found strong evidence for an interaction between the pre-saccadic preview stimulus and the post-saccadic target as early as 50 ms (Experiment 2) or 90 ms (Experiment 1) into the new fixation. These findings suggest that visual stability may involve three temporal stages: prediction about the saccadic target, integration of pre-saccadic and post-saccadic information at around 50-90 ms post fixation onset, and post-saccadic facilitation of rapid categorization.

1. Introduction

Visual perception is surprisingly stable despite being interrupted by saccadic eye movements about three times per second. One source of visual stability may be the integration of pre- and post-saccadic visual information (Helmholtz, 1867; Melcher, 2011; Wurtz, 2008). Recent gaze-contingent experimental designs have revealed that orientation (Ganmor et al., 2015; Wolf and Schütz, 2015; Zimmermann et al., 2017), object size (Valsecchi and Gegenfurtner, 2016), visual motion (Fabius et al., 2016), and even whole-object information (Castelhano and Pereira, 2017; Schut et al., 2016) are integrated across saccades in a

statistically optimal fashion that takes into account the relative reliability of pre-saccadic and post-saccadic input (Ganmor et al., 2015; Herwig, 2015; Wolf and Schütz, 2015). Nonetheless, the time-course of trans-saccadic perception and, in particular, the contents of perception immediately after fixation-onset remain controversial (for review, Melcher and Morrone, 2015).

Here, we investigated the time-course of trans-saccadic perception with combined EEG and eye-tracking (Huber-Huber et al., 2016; Kovalenko and Busch, 2016). Using a similar methodology, reading research has discovered a *preview positivity* in the fixation-locked potentials (FRP) starting at around 140-200 ms in which the evoked response is more

---

positive after valid as compared to invalid parafoveal previews (Dimigen et al., 2012; Kornrumpf et al., 2016; Niefind and Dimigen, 2016), suggesting that pre- and post-saccadic information about the target word are compared and integrated as soon as 140-200 ms after fixation onset.

Here we investigated whether the preview positivity known from reading research is also elicited by non-word stimuli, namely by faces. One advantage of using face stimuli is that the time course of face processing has been extensively studied (e.g. Bentin et al., 1996). In Experiment 1, participants made saccades to peripheral face stimuli. During the saccade, the orientation of the face (upright, inverted) could change (invalid preview) or remain the same (valid preview). After the saccade, participants reported by button press whether the post-saccadic target face was slightly tilted to the left or right. If the preview positivity observed in reading reflects a general trans-saccadic integration mechanism, a change in the FRP component around 200 ms, as found with reading, should be elicited by a valid preview of the target face. However, we hypothesized that faces might show an earlier preview effect than words (Edwards et al., 2018), possibly influencing the N170 ERP index of face processing (Buonocore et al., 2019).

The N170 has been closely associated with face processing in the fusiform gyrus and lateral occipitotemporal cortex (Rossion and Jacques, 2011; for review) and is known to be sensitive to contextual effects. For example, repeated presentation of faces reduces the N170 component (Caharel et al., 2009; Ewbank et al., 2008) and inverting faces generates a larger and sometimes later N170. This face inversion effect in the N170 is considered to reflect the configural or structural encoding of faces, supporting detection of face stimuli rather than more detailed resolution of face identity (Bentin et al., 1996; Eimer, 2000; Eimer et al., 2010; Itier and Taylor, 2004a, 2004b; Rossion et al., 2000; Towler et al., 2012; Watanabe et al., 2003). However, face inversion effects also emerge when faces are not explicitly present but can be inferred from context (Brandman and Yovel, 2012).

Trans-saccadic preview effects are usually expressed as more pronounced neural responses in invalid compared to valid conditions (Dimigen et al., 2012; Näätänen and Kreegipuu, 2011). As such they can be interpreted in terms of prediction errors in predictive coding frameworks (Friston, 2010, 2005; Friston and Kiebel, 2009; Giordano et al., 2009; Stefanics et al., 2014) and in current frameworks of predictive perception (De Lange et al., 2018). With respect to trans-saccadic perception, the interpretation of the preview effect as a predictive process is particularly intriguing, because one explanation for visual stability is that upcoming foveal visual input is predicted based on pre-saccadic peripheral information and a copy of the motor command (Cavanaugh et al., 2016; Friston et al., 2012; Melcher and Colby, 2008; Wurtz, 2008). Finding predictive preview effects would therefore foster the prediction hypothesis of visual stability.

Setting out to test the predictive nature of the trans-saccadic preview effect, in Experiment 2, we asked whether the trans-saccadic preview effect reflected a relatively long-term predictive process that extends across multiple trials. We manipulated the proportion of valid and invalid trials to generate blocks with mostly valid (66.6% valid) and mostly invalid (33.3% valid) previews. Proportion manipulations have successfully demonstrated the predictive nature of sensory processing (Grotheer et al., 2014; Kovács et al., 2012; Mayrhauser et al., 2014; Summerfield et al., 2011, 2008), with the rationale that a more frequent event is more expected than a less frequent event and, therefore, elicits a reduced neural response. Thus, if the preview effect reflects a predictive process that is sensitive to the task context, it should become smaller in the mostly invalid and larger in the mostly valid block.

2. Materials & Methods

2.1. Participants

Twenty volunteers participated in each experiment in return for a monetary reimbursement, with no overlap in participants between the two experiments. All participants provided written informed consent and reported normal or corrected-to-normal visual acuity that was additionally confirmed by an eyesight test using a Snellen chart. In Experiment 1, two participants had to be excluded due to poor performance in the tilt discrimination task. Of the remaining 18 participants, 16 were right-handed, 7 were male, and their mean age was 24.3 years (range: 19-30 years). In Experiment 2, one participant had to be excluded because of a technical problem during EEG data collection. Of the 19 remaining participants, 16 were right-handed, 6 were male, and their mean age was 25.0 years (range 20–40 years). The procedures of both experiments were approved by the local ethics committee.

2.2. Stimuli

Stimuli were presented on a VIEWPixx/EEG monitor (VPixx Technologies Inc., Canada) at 120 Hz screen refresh rate and 1920 × 1080 display resolution. The experiment was programmed in Matlab (version 2014b, The Mathworks Inc.) using the Psychophysics toolbox (Brainard, 1997; Pelli, 1997). For Experiment 1, 42 face images were taken from the Nottingham face database (http://pics.stir.ac.uk/zips/nottingham.zip) as well as from the Faces 1999 (Front) dataset (http://www.vision.caltech.edu/archive.html), with half of the images being female faces and the other half male faces. For Experiment 2, we selected a set of 16 face images only from the Nottingham face database, with half of the images showing female faces and half male faces. The face images in this reduced set were more uniform concerning the distribution of facial features like eyes, nose, and mouth across images.

For the face images of both experiments, a circular mask with a diameter of 2.88° was centered at the tip of the nose and the image was sized to contain the internal facial features. Face images were centered bilaterally at ±8° eccentricity from the screen center. For each original face image, we generated a phase-scrambled counterpart that was presented as a transient (for the duration of 2 display frames, i.e. 16.7 ms) during the saccade to match the level of intrasaccadic visual change of the display between the valid and invalid preview conditions. In order to equate low-level image features that could otherwise confound the EEG signal, stimuli were matched with the SHINE toolbox (Willenbockel et al., 2010). Specifically, we used the function *histMatch* with the mask option to match the luminance histogram of all face cut-outs and their scrambled counterparts to the average histogram of all face cut-outs within each of the two experiments.

2.3. Procedure

Each trial started with a placeholder display consisting of a fixation cross (0.5° × 0.5°) at the screen center and two white rings (width 1 pixel) framing the position of the upcoming faces (Fig. 1A). In Experiment 1, one white ring appeared on either side of the fixation cross (as illustrated in Fig. 1A), in Experiment 2, only one ring appeared to the left of fixation (not illustrated). Stable fixation within an area of 2° around the screen center for 1 s triggered the preview display. In Experiment 1, the preview display contained two faces, one at either side from fixation; in Experiment 2, there was only one face to the left of fixation. The face images replaced the placeholder rings. Once the eye tracker detected a stable fixation at the center of the preview display for 500 ms, the color cue was presented. In Experiment 1, the fixation cross turned either blue or green indicating the saccade direction (color-to-direction assignment counterbalanced across participants). In Experiment 2, the fixation cross turned grey, prompting for a saccade to the single face on the left. Participants were instructed to respond as quickly and accurately as possible to the cue by making one single eye-movement to the corresponding face stimulus. Saccade onsets were detected online (see section *EEG and eye-tracking data recording* for details), and upon detection, a scrambled version of the preview face was presented for two frames (16.7 ms); in Experiment 1, the faces on both sides were scrambled. The transient occurred no more than 3.5 frames (~30 ms) after saccade onset, with the
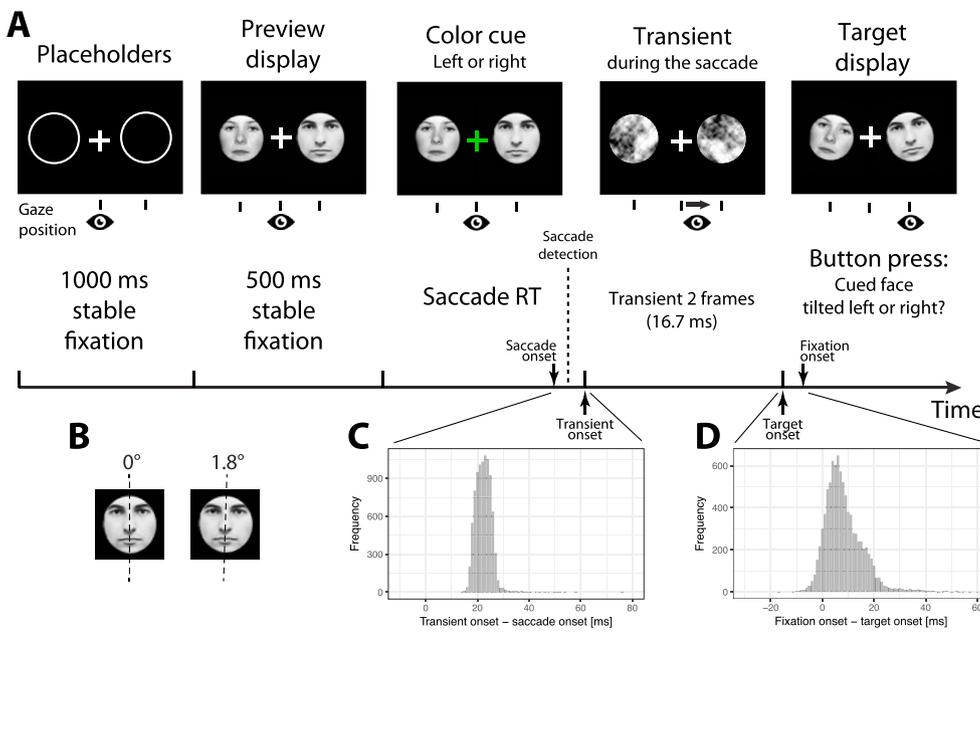
Fig. 1. Panel A. Procedure in Experiment 1. A stable fixation for 1000 ms triggered the *Preview* display. Further fixation for 500 ms then triggered the color cue (e.g. green left/blue right, counterbalanced across participants) indicating the required saccade direction and, thus, the target face. Both the target (cued) face and non-target face (opposite side) could be either upright or inverted, and could both either change orientation of remain the same across the saccade. During the saccade, scrambled versions of the faces were presented as transients. The transient was replaced by the target display after two frames. The target display contained both target and distractor faces with additional slight tilt (left/right, amount of tilt is exaggerated in panel A). Panel B shows the true to scale target face tilt of 1.8°. The direction of this tilt had to be reported by button press upon fixation onset. Panel C illustrates the speed of the online saccade detection. In most trials, the transient was presented less than 25-30 ms after saccade onset. The timing of target onset and fixation onset is illustrated in panel D. Fixation onset was most of the time after target onset. Timeline, stimulus size, and target face tilt in panel A are not drawn to scale.

delay reflecting the computational requirements of saccade detection and the screen refresh rate (Fig. 1C). Given a total saccade duration of around 40-60 ms, the target face was presented before fixation onset in most trials (Fig. 1D). The purpose of this transient was to roughly equalize the amount of change in the display across all conditions.

During the saccade the faces could change their overall orientation from upright to inverted (or vice versa) or they could remain the same. In Experiment 1, all possible combinations of target and non-target face orientations and changes were realized once with each individual target face, yielding a total set of 672 trials (168 per cell in the crossing of *Preview* [valid, invalid] and *Target Face* [upright, inverted] conditions; Fig. 2A). In Experiment 2, which employed a smaller set of face images, all possible combinations of target orientations and changes were repeated 16 times for each face. In addition, to investigate whether the preview effect found in Experiment 1 reflected active predictions accumulating across blocks of trials, Experiment 2 consisted of two blocks, one containing mostly valid trials (66.6% valid, 33.3% invalid) and the other one containing mostly invalid trials (33.3% valid, 66.6% invalid) (Fig. 2B). We were interested whether the preview effect - the difference in the dependent variables between invalid minus valid trials - would be

larger in the mostly valid block and smaller in the mostly invalid block (Fig. 3). Block order was counterbalanced across participants.

Experiment 2 thus comprised 1024 trials (with either 171 or 85 per cell in the crossing of *Preview* [valid, invalid], *Target face* [upright, inverted], and *Proportion* [mostly valid, mostly invalid] conditions). For instance, in the mostly valid block, there were 171 valid trials with target upright, 171 valid trials with target inverted, 85 invalid trials with target upright, and 85 invalid trials with target inverted. Importantly, the proportion manipulation was not mentioned to the participants at any point.

In addition to its main orientation (upright or inverted), each target face was slightly tilted (1.8°) either to the left or right, counterbalanced across trials. The non-target face in Experiment 1 had the same amount of tilt as the target face (on the other side of fixation), but its direction (left or right) was random. The target face tilt direction had to be reported by the participants via a computer keyboard with the left and right index finger after they had made an eye-movement to the target face. Fig. 1B shows the true-to-scale tilt of 1.8° which was hard to see even in the fovea but sufficient for above-chance performance (mean error rates per condition between 15% and 20%, cf. section 3.1.). The purpose of the tilt
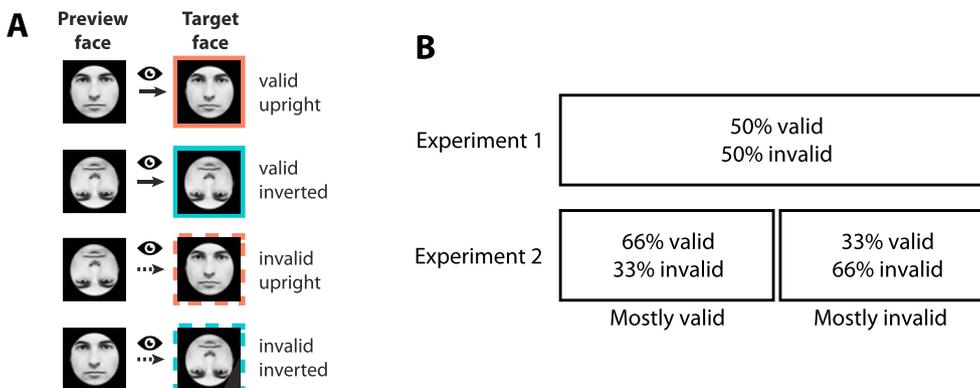

Fig. 2. Panel A shows the four possible preview and target face orientation conditions. Both *Preview orientation* and *Target orientation* could be upright or inverted leading to in total four conditions, two of which contained a valid preview (preview orientation and target orientation matched) and two an invalid one (preview orientation and target orientation did not match). Panel B shows the proportion of valid and invalid trials in Experiment 1 and 2. In Experiment 1, valid and invalid trials occurred at a frequency of 50% throughout the experiment. Experiment 2 consisted of two blocks, one with mostly valid (66.6% valid, 33.3% invalid) and one with mostly invalid trials (33.3% valid, 66.6% invalid). Block order was counterbalanced across participants.
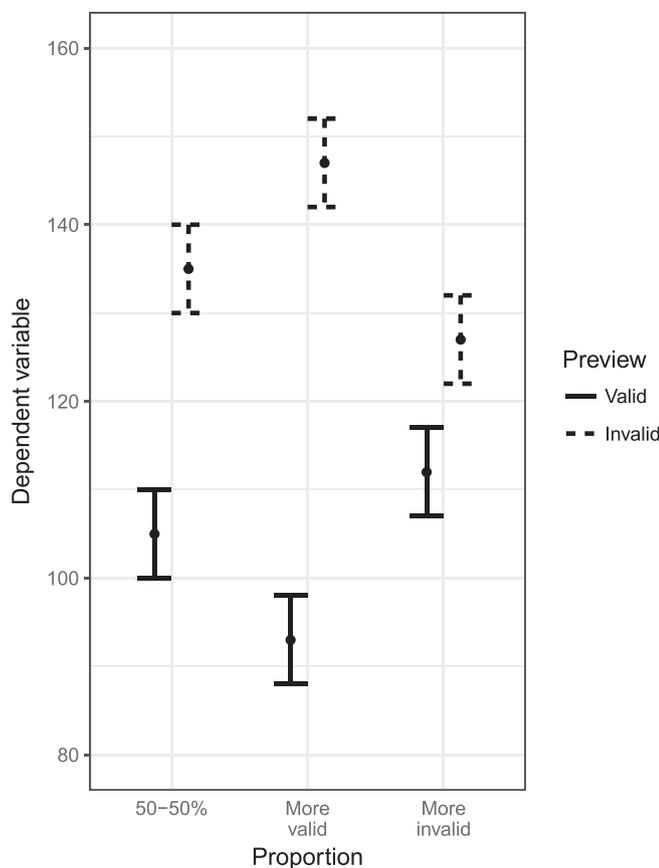
Fig. 3. Illustration of the logic of the proportion manipulation to determine the predictive nature of the preview effect (difference on the y-axis between valid, solid, and invalid, dashed, conditions). If the preview effect is predictive, a block with more valid trials is expected to increase the preview effect, and a block with more invalid trials is expected to decrease the preview effect.

discrimination task was to ensure that participants paid attention to the target face and gave a response that was orthogonal to all experimental manipulations. In fact, the preview images were not tilted, making them task-irrelevant for the perceptual tilt discrimination response. Correct saccades (end point at least within 2.16° of the target face center) were detected online, and participants received feedback in case of incorrect response or if the recorded gaze position was too far from the expected saccade start or end locations. Before data collection, the eye-tracker was calibrated with a default 5-point rectangular grid. The eye-tracker was manually recalibrated when it failed to correctly track gaze position, that is, when the gaze position suggested that the participant was not following the instructed gaze procedure anymore.

2.4. EEG and eye-tracking data recording

The electroencephalogram (EEG) was recorded with a 64-channel DC system (Brain Products GmbH, software: BrainVision Recorder version 1.21) in an electromagnetically shielded booth. Sixty-three electrodes were placed at a subset of the locations of the 10-10 system: Fp1, Fpz, Fp2, AF7, AF3, AF4, AF8, F9, F7, F5, F3, F1, Fz, F2, F4, F6, F8, F10, FT7, FC5, FC3, FC1, FCz, FC2, FC4, FC6, FT8, C5, C3, C1, Cz, C2, C4, C6, T8, TP7, CP5, CP3, CP1, CPz, CP2, CP4, CP6, TP8, P7, P5, P3, P1, Pz, P2, P4, P6, P8, PO9, PO7, PO3, POz, PO4, PO8, PO10, O1, Oz, and O2. The right mastoid served as online reference and electrode AFz was used as ground. Eye-movement data was recorded by a desktop-mounted Eyelink 1000 video-based eye-tracker (SR Research, Ontario, Canada). Default settings for saccade detection were used (velocity threshold 35°/s, acceleration threshold 9500°/s²). The online saccade detection that triggered the

intrasaccadic scrambled transient (see *Procedure*) was, however, based on a custom-made algorithm, since the default saccade start events were not transferred quickly enough from the eye-tracking host computer to the experiment workspace in Matlab. We set the heuristic filter option of the eye-tracker to level 2 in order to receive cleaner gaze position data, despite the minimal additional delay introduced by the higher filter level. A gaze position difference of 0.18° between two subsequent samples, converted to screen pixels depending on individually measured viewing distance of each participant, triggered presentation of the scrambled transient at the next possible screen refresh. This procedure resulted in quick and satisfactory saccade detection in most trials (cf. Fig. 1C).

Both eye-tracking and EEG data were recorded at 1000 Hz. Trigger signals were sent to both data acquisition systems by means of a parallel port splitter cable. The trigger signals were used offline to synchronize both data streams for subsequent analysis.

2.5. EEG and eye-tracking data analysis

EEG and eye-tracking data were processed in Matlab (version R2016b, The Mathworks Inc.) using EEGLAB (version 14.1.1, Delorme and Makeig, 2004). The eye-tracking data was synchronized with the EEG by means of the EYE-EEG toolbox (version 0.81, Dimigen et al., 2011). After synchronization, the synchronized signals were down-sampled to 250 Hz. The EEG was then low-pass filtered (Hamming windowed sinc FIR filter, edge of the passband 40 Hz, transition bandwidth 10 Hz, -6 dB cutoff frequency 45 Hz), and re-referenced to average reference (Hinojosa et al., 2015). The EEG data was then visually inspected for major artifacts. Portions of data with severe artifacts were removed and bad channels were spherical-spline interpolated.

In order to correct for eye movement artifacts in the EEG, we applied independent component analysis (ICA; Makeig et al., 1996). Eye-movement related components were determined based on the variance ratio of component activation during periods of eye-movements (blinks and saccades) versus periods of fixations (Plöchl et al., 2012). ICA was conducted in a separate processing pipeline containing an additional high-pass filter (Hamming windowed sinc FIR, edge of the passband: 1 Hz, −6 dB cutoff frequency: 0.5 Hz) that was applied after down-sampling and before low-pass filtering (Dimigen, 2018; Winkler et al., 2011). The ICA algorithm was Infomax (Bell and Sejnowski, 1995) with the "pca" option activated to account for the reduced rank of some of the datasets that contained interpolated channels. The ICA results (sphere and weights) were transferred to the corresponding datasets in the original processing pipeline, which lacked a high-pass filter (cf. Acunzo et al., 2012). Components were then rejected if the mean variance of their activity time course during eye-movement periods was 10% greater than the mean variance during fixation periods (Plöchl et al., 2012; Dimigen, 2018).

In both experiments, we extracted epochs of interest time-locked to the target fixation. Target fixation epochs were extracted from −200 to 600 ms around the onset of the first face fixation. Baseline correction was conducted with respect to the 200 ms period before onset of the preview display. This approach was adopted for two reasons: first, to compare the post-saccadic activity to a period in which there was no visual input, and, second, to prevent possible residual eye-movement-related activity from confounding the baseline. In Experiment 2, we also extracted epochs of interest aligned to the onset of the preview display, from −200 to 800 ms with respect to preview display onset, with the baseline defined as the interval from −200 to 0 ms prior to preview display onset.

Only trials with correct responses and trials in which participants had followed the gaze instructions in the experimental procedure were included in the analysis. These were trials in which participants kept a stable fixation within 2° of the screen center, made no saccades before cue onset, and the saccade endpoint was within 2.16° of the target face center. If the target had not been presented before fixation onset, due to a delay in saccade detection, the time difference between fixation onset and target onset was less than 20 ms (see Fig. 1D and Procedure for

details), which is largely within the time course of saccadic suppression (Benedetto and Morrone, 2017; Bremmer et al., 2009; Diamond et al., 2000). This restriction was disregarded in Experiment 2 for the preview-locked analysis only, because this analysis focused on the time period before the saccade and disregarding this criterion increased the number of available trials. Finally, trials with very fast and very slow responses in the tilt discrimination task were excluded by a median absolute deviation filter with a conservative criterion of 3 (Leys et al., 2013).

In Experiment 1, these strict criteria led to acceptance of a median number of 104 trials (range 58–139 across participants) per cells of the experimental design (*Preview* × *Target Orientation*). In the FRP analysis of Experiment 2, the median number of accepted trials was 78 (range 32–165) per cell of the design (*Preview* × *Target Orientation* × *Proportion*). For the preview-locked analysis of Experiment 2, the median number was 79, and the range was the same. The extended range in Experiment 2 compared to Experiment 1 was due to the proportion manipulation, which lead to an unbalanced number of trials across cells of the design.

To determine how the pre-saccadic preview affected processing of the post-saccadic target face, we investigated the time course of *Preview orientation* (upright, inverted) and *Target orientation* (upright, inverted) effects in the EEG with a whole-scalp Bayes factor analysis. ERP components are known to differ across tasks, and since we used a novel gaze-contingent task, such an analysis reduces the risk of false positive findings (Luck and Gaspelin, 2017). Note, that the same conditions resulting from the factors *Preview orientation* (upright, inverted) and *Target orientation* (upright, inverted) can be modelled equally well by either of the factors *Target* or *Preview orientation* (upright, inverted) together with a *Preview* factor (valid, invalid) that indicates whether the target and the preview face were of the same (valid) or different (invalid) orientation.

Experiment 1 also included the factor *Cue Direction* (left, right; synonymous with saccade direction) and, for lateral electrodes, also the factor *Laterality* (contra, ipsi; with respect to cue direction). To create the *Laterality* factor, EEG data from trials with saccades to the left were swapped across hemispheres in order to assign left hemisphere electrodes to the contralateral, and right hemisphere electrodes to the ipsilateral condition. For instance, the signal at electrode PO7 was assigned the label *ipsilateral* for leftward saccade trials and the label *contralateral* for rightward saccades trials. The signal at electrode PO8 was treated in the opposite way. With a visually balanced display of one face at either side of the screen, the face at the future target location, i.e. the preview face, projects primarily to the contralateral hemisphere. Analyzing the data with the laterality factor ensured that any lateralized preview-related activity could be captured by our design. The alternative would have been to keep the signal at corresponding electrodes separate (e.g. PO7 separate from PO8), which would have meant averaging activity ipsilateral to the preview face with activity contralateral to the preview face, and that might have cancelled out any lateralized preview-related effects. In contrast to Experiment 1, Experiment 2 omitted the factors *Cue Direction* and *Laterality*, because there was only one target face to the left to which saccades were directed, but instead it included the factor *Proportion* (mostly valid, mostly invalid). For Experiment 2, we additionally analyzed the data time-locked to the preview display in order to determine any pre-saccadic expectation effects introduced by the proportion manipulation.

The preview-display locked analysis of the EEG data revealed an unexpected result, with the face inversion effect in the N170 triggered by the preview display occurring later than the face inversion effect triggered by the target display. We tested the reliability of this delay by analyzing onset latencies of the N170 face inversion effect. Since this was a post-hoc analysis, this result might be less reliable. In addition to the whole-scalp Bayes factor, we also computed repeated measures ANOVAs on average ERPs at selected electrode sites and for time-windows of main interest to further consolidate the results.

2.6. Whole-scalp analysis

At each electrode and time point, we computed a Bayes factor (BF) based on the average EEG voltage across trials per participant and condition. We used the BayesFactor package (version 0.9.12–2) in R (R Core Team, 2013) with fixed-effect priors set to the default Cauchy distribution at location 0 and scale 0.5. This prior can be verbally expressed as expectation of a medium-sized effect with smaller effects being more likely than larger effects (Rouder et al., 2009). In contrast to null-hypothesis significance testing, the Bayes factor provides a measure of graded evidence for the presence versus absence of an effect (Dienes, 2016; Rouder et al., 2016; Wagenmakers, 2007). In line with common practice, we consider a BF greater than 3 as positive evidence, a BF lower than 1/3 as negative evidence, and a BF between 1/3 and 3 as non-decisive (Raftery, 1995).

To obtain a BF for a main or an interaction effect in a multifactor design, such as in the present study, it is advisable to calculate the so-called BF *across matched models*. This is because the BF is a likelihood ratio that results from comparing two models, which is usually the likelihood of the data given the alternative hypothesis/model divided by the likelihood of the data given the null hypothesis/model. A multifactor design offers many pairs of models with one model containing the effect of interest and the other not. Thus, there are many possible likelihood ratios that could be considered as providing the BF for a certain effect. The most straightforward way to solve this problem is to compute the sum of the likelihoods of all of the models with the effect of interest and divide it by the sum of the likelihoods of all of the corresponding models without the effect of interest. Models containing higher-order interactions with the effect of interest are disregarded. This procedure is, for instance, implemented in the software JASP (JASP Team, 2018).

3. Results

3.1. Experiment 1: Valid peripheral preview improves post-saccadic tilt discrimination performance

We analyzed manual response times in the tilt discrimination task only for those trials that entered the EEG analysis, which also excludes tilt discrimination errors. Error trials were, however, included in the error rate analysis, which still excluded trials with incorrect saccades (see *Methods*). For both computations the design contained three factors: *Target Orientation* (upright, inverted), *Preview* (valid, invalid), and *Cue Direction* (left, right; equivalent with saccade direction). Response time was measured from cue onset, which means that it included saccade latency. Saccade latency was on average 414 ms and did not differ across conditions, all $Fs < 1.55$, all $ps > .232$, all BFs < 0.33, except for the Preview x Target Orientation x Cue Direction interaction which had a Bayes factor slightly above the 0.33 threshold but still below 1, $F(1,17) = 2.25$, $p = .152$, BF = 0.42.

As expected, a valid preview led to on average shorter response times than an invalid preview (valid 1180 ms, invalid 1209 ms), $F(1,17) = 14.54$, $p = .001$, BF = 7.52 (Fig. 4A) which is in line with the behavioral preview benefit effect in reading research (Rayner, 1975; for a review see Schotter et al., 2012). Error rates were the same in both preview conditions (valid 17%, invalid 18%), $F(1,17) = 1.35$, $p = .261$, BF = 0.28 (Fig. 4B). Performance was also affected by target face orientation. Upright target faces led to a faster response than inverted target faces (1163 ms versus 1227 ms), $F(1,17) = 22.48$, $p < .001$, BF > 100. Upright faces were also less error prone (15%) than inverted ones (20%), $F(1,17) = 20.68$, $p < .001$, BF > 100. This effect was, however, not of primary interest in the current study.

The ANOVA also showed an interaction of *Preview* and *Cue Direction* in the error rates, $F(1,17) = 8.80$, $p = .009$. This interaction suggested a larger preview effect for left side targets than for right side targets. However, a BF of 0.66 prevented us from drawing strong conclusions.
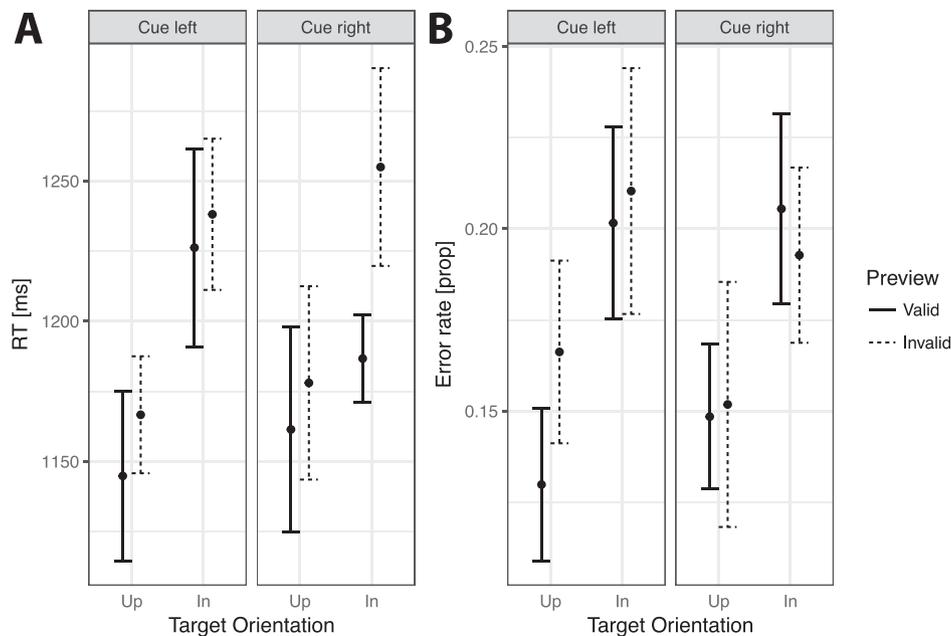
Fig. 4. Mean response times (panel A) and error rates (panel B) in the tilt discrimination task in Experiment 1, split by the factors *Cue Direction*, *Target Orientation*, and *Preview*. Participants were faster in valid (solid) than in invalid preview conditions. Target orientation also affected the response: Participants responded faster (panel A) and made fewer errors (panel B) in trials with upright (Up) compare to with inverted (In) target faces.

3.2. Experiment 1: Valid peripheral preview reduces the N170 amplitude in the FRP

Results of the FRP whole-scalp Bayes factor analysis are illustrated in Figs. 5 and 6. Fig. 5 shows the BF for the theoretically most relevant effects of *Preview Orientation* (panel A, aka Preview × *Target Orientation* interaction), *Target Orientation* (panel B), and the Preview effect (panel C, aka *Preview Orientation* × *Target Orientation* interaction). The ERPs corresponding to these effects are illustrated in panel D. Note that the *Preview Orientation* (upright, inverted) main effect is expressed as a *Preview* × *Target Orientation* interaction.[1] Fig. 6 shows the remaining and less theoretically important effects.

As can be seen from Fig. 5, the initial phase of the FRP response already showed some evidence for an influence of the orientation of the preview face (panel A), which became decisively positive (BF > 3, color-coded in blue within white contour lines) from around 110 to 170 ms post fixation onset. During this relatively early period after fixation onset the preview face was no longer presented on the screen but instead had been replaced by the target face, which could have had a different orientation than the preview face. Nevertheless, an inverted preview face led to a more negative EEG response than an upright preview face at posterior-lateral electrodes (see panel D). This effect could reflect a mechanism relevant for the experience of visual stability, since it indicates that information about the pre-saccadic preview influenced neural processing in this time period of around 110-170 ms. In other words, immediately after the fixation, the EEG signal initially reflected

what was perceived before the saccade and would be expected to be perceived after the saccade, until new post-saccadic information was incorporated (Mirpour and Bisley, 2016). For face orientation this updating process apparently happened at around 170 ms, which co-incides with the timing of the face-selective N170 component.

Almost exactly at 170 ms the main influence on the EEG signal switched from the preview face to the target face (cf. Fig. 5A–B) which elicited a more negative response when inverted compared to when it was upright (Fig. 5D). This modulation perfectly matches the classic N170 face inversion effect (Bentin et al., 1996; Eimer, 2000; Eimer et al., 2010; Itier and Taylor, 2004a, 2004b; Rossion et al., 2000; Towler et al., 2012; Watanabe et al., 2003). We therefore consider this target orientation effect around 170-220 ms post fixation as a modulation of the fixation-locked N170 component, the fN170.

Most importantly, for a period of about 80 ms before and after the crucial time point of 170 ms, the preview orientation and target orientation factors interacted (Fig. 5C), showing a more pronounced neural response when the preview face and target face orientations matched (valid preview) compared to when they did not match (invalid preview) (Fig. 5D). This finding is consistent with theories of trans-saccadic integration that posit that information about the saccadic target influences post-saccadic processing of that target in the new fixation (for review see Melcher, 2011). As can be seen from Fig. 5D, the fN170 component in particular was more pronounced in invalid (dashed lines) than in valid preview (solid lines) conditions, which is consistent with the idea of a trans-saccadic prediction error. The role of prediction was further explored in Experiment 2.

As can be seen in Fig. 5, panels A and D, the factors *Preview* and *Target Orientation* interacted again from around 320 ms post fixation for a duration of about 80 ms in particular at central parietal electrodes. The target orientation effect here consisted in a more negative deflection for inverted compared to upright target faces and this face inversion effect was larger for invalid than for valid preview conditions. This interaction likely reflects increased processing of the target face orientation in invalid than in valid preview conditions – after an invalid preview, the target face requires more in-depth processing of the critical features related to face processing – which appears intuitively plausible given the literature on the P300 component (e.g. Polich, 2011).

---

[1] We checked the equivalence of the *Preview Orientation* main effect and the *Preview* × *Target Orientation* interaction explicitly with two ANOVAs computed on the average amplitude within 300–400 ms post fixation onset at electrode pair PO7/8. One ANOVA contained the effect of *Preview Orientation* whereas the other ANOVA coded the same data with the effect of *Preview* instead. The first ANOVA showed a main effect of *Preview Orientation* with the values $F(1,17) = 4.39$, $p = .051$. The second ANOVA showed a *Preview* × *Target Orientation* interaction with exactly the same values $F(1,17) = 4.39$, $p = .051$. Besides that, the main effect of *Target Orientation* was also exactly the same for both ANOVAs, $F(1,17) = 8.92$, $p = .008$. Clearly, the *Preview Orientation* main effect translates into a *Preview* × *Target Orientation* interaction, and vice versa.
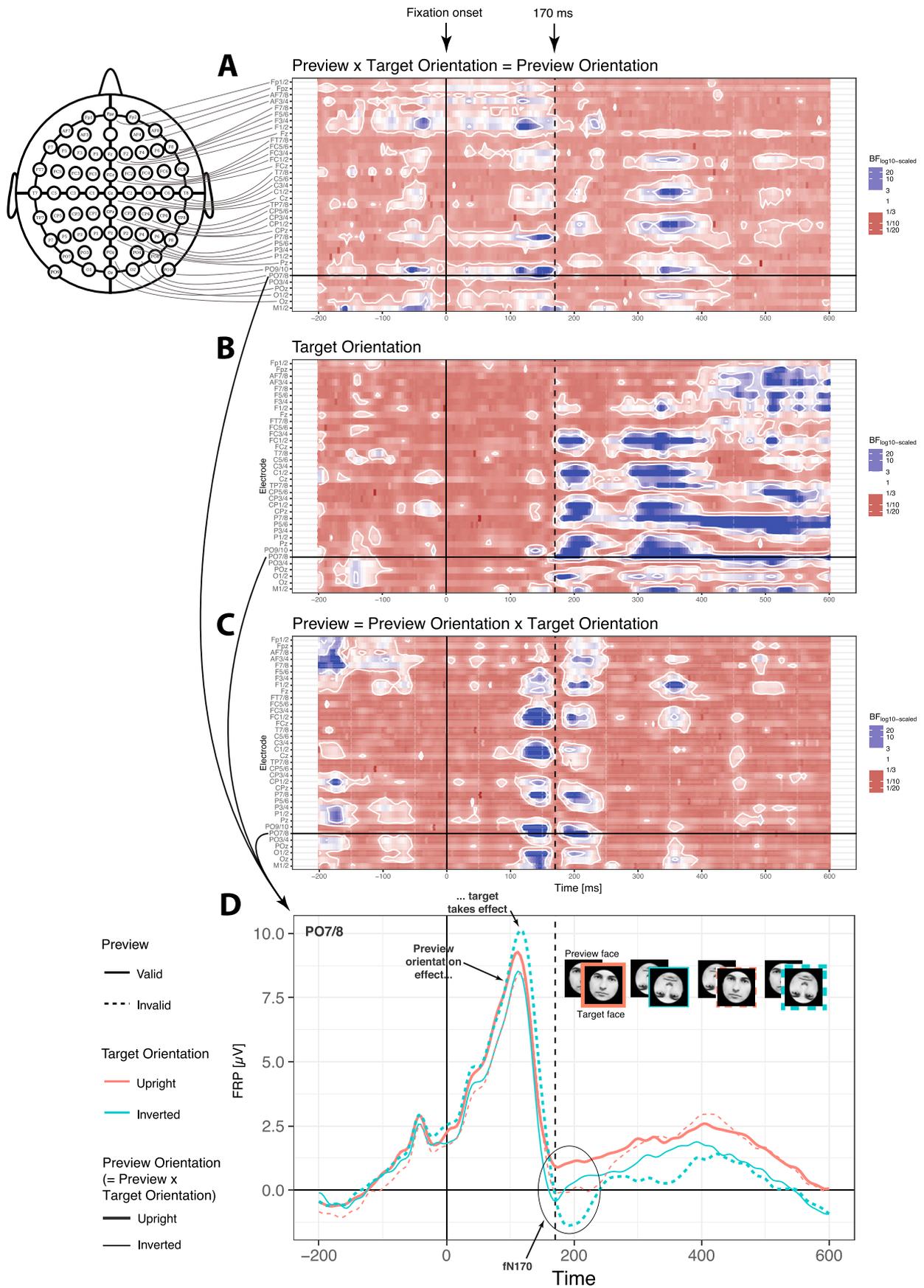
(caption on next page)

Fig. 5. Whole-scalp Bayes factor (BF) analysis of the fixation-related potentials (FRP) to the target face (panels A–C). Panel D illustrates the corresponding ERPs at electrode pair PO7/8. Each horizontal row of panel A–C represents the time-course of the BF for one contra-ipsilateral electrode pair, sorted from frontal (top) to posterior (bottom) sites and within this order further from lateral (top) to medial (bottom) sites. Values greater than 3 (blue) denote positive evidence, values less than 1/3 (red) negative evidence. Values in-between are indecisive (white). The thresholds 3 and 1/3 are indicated by two-dimensional white contour lines. The vertical dashed line at 170 ms only serves as visual guide and does not indicate any event in the experiment. Panel A shows the *Preview × Target Orientation* interaction, aka *Preview Orientation* main effect. From ca. 100 ms post fixation onset to 170 ms the orientation of the preview face dominated the posterior lateral EEG signal (see also panel D). Evidence for this effect became positive again between ca. 300–400 ms primarily at central-parietal sites. Panel B illustrates the main effect of *Target Orientation*. Evidence for this effect became positive from ca. 170 ms post fixation-onset at lateral posterior and some central sites and, after some decrease in evidence from ca. 250–300 ms extended throughout the post-saccadic time-window. The corresponding face inversion effect in the fN170 is illustrated in panel D. Panel C shows evidence for the crucial *Preview* effect, aka *Preview Orientation × Target Orientation* interaction. In time windows of ca. 50 ms before and after 170 ms the EEG response was more pronounced in valid (preview orientation and target orientation matched) compared to invalid (no match) conditions. The ERPs in panel D show this effect in the fN170 component at electrode pair PO7/8. Note that baseline correction was conducted with respect to the time window −200 to 0 ms before preview display onset which is outside the plotted time period (cf. Fig. 1).

As can be seen from Fig. 6, with one exception (three-way interaction with *Cue Direction*, Fig. 6H), the *Preview* and *Target Orientation* factors did not interact with other factors. The interaction with *Cue Direction* showed sufficient positive evidence before and around the time of the saccade and suggested that the *Preview × Target Orientation* interaction – which is the statistical reflection of the *Preview Orientation* effect – consisted of more negative EEG for inverted compared to upright preview faces, which was more pronounced for saccade-right trials than for saccade-left trials (direction of effects not illustrated here). Given the posterior lateral distribution of this effect (electrodes O1/2, PO9/10), and the time periods before and around the time of the saccade, this effect might be

attributed to saccade-related perceptual processes.

Additional effects of less theoretical significance were identified in our analyses, including a main effect of *Cue Direction* (Fig. 6A), and the substantial effects of *Laterality* (Fig. 6B) as well as the *Laterality × Cue Direction* interaction (Fig. 6G). The *Cue Direction* effect indicated evidence for differences between right side and left side saccade trials at posterior lateral electrodes from ca. 100–160 ms and at central electrodes from during the saccade to 170 ms post fixation (Fig. 6A). The *Laterality* effect showed strong evidence for widespread effects across the whole post-saccadic time period (Fig. 6B). Finally, *Laterality* and *Cue Direction* showed a pronounced interaction across several electrode sites and
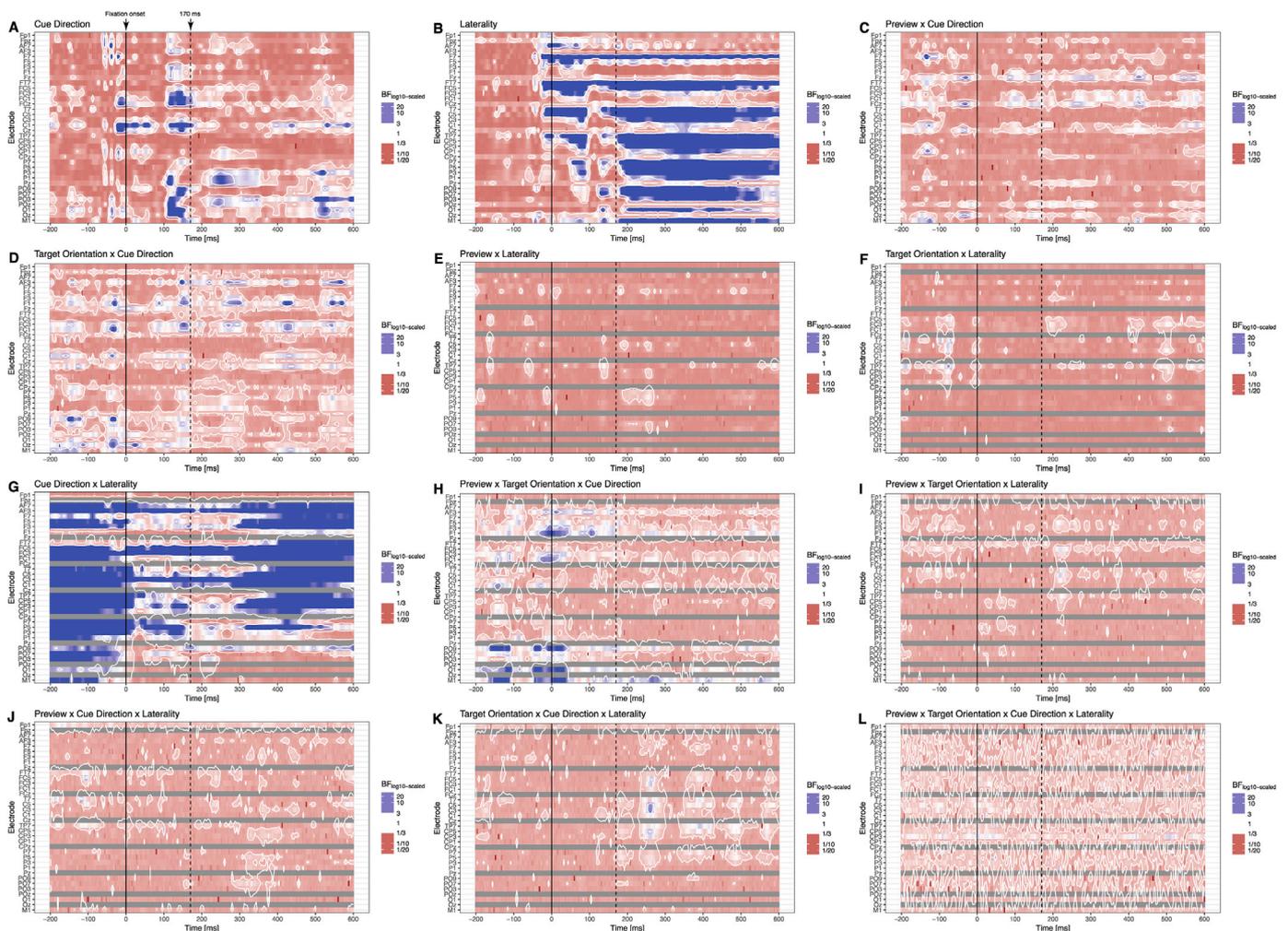

Fig. 6. Whole-scalp Bayes factor (BF) for all the remaining main and interaction effects of Experiment 1 not illustrated in Fig. 5. Importantly, the *Preview* and *Target Orientation* effects did not interact with other factors in particular not in the spatio-temporal window of the fN170 preview effect at lateral posterior electrodes ca. 50 ms before and after the 170 ms time stamp.

across the whole analysis time window (Fig. 6G). Such laterality effects might be related to face processing differences between hemispheres (Frässle et al., 2016; Schweinberger et al., 2004), specifically, a stronger involvement of right posterior parietal cortex in oculomotor control or remapping processes (for review see Pisella et al., 2011; Prime et al., 2011), or some other factor beyond the scope of the current study. These factors were modelled in the analysis in order to control for potential interactions with the preview and target orientation effects, which were of central theoretical interest here.

3.3. Experiment 1: ANOVA results in the fN170 time window in line with the whole-scalp analysis

To provide a statistical assessment of the main results from a frequentist perspective, we computed repeated measures ANOVAs on average ERPs at electrode pair PO7/8, which typically shows the most pronounced N170 effects (Hinojosa et al., 2015), in the time window from 165 to 250 ms. This time window is later than the one usually adopted in ERP studies of the N170 (Bentin et al., 1996), but is appropriate given the extended N170 observed in the invalid preview conditions of our experiment (cf. Fig. 5). To assess the later central-parietal *Preview × Target Orientation* interaction, we additionally computed a repeated measures ANOVA at electrode CPz for the later time window of 320–400 ms.

The ANOVA results were in line with the evidence from the whole-scalp BF analysis. The ANOVA showed clear main effects of *Preview*, $F(1,17) = 36.55$, $p < .001$, and *Target Orientation*, $F(1,17) = 8.50$, $p = .010$, which corroborated the more pronounced N170 in invalid compared to valid preview conditions and the more pronounced N170 for inverted compared to upright target faces. The *Target Orientation × Cue Direction* interaction approached marginal significance, $F(1,17) = 4.01$, $p = .062$, but the corresponding BF = 0.30 suggested that the evidence for this effect is negative. We do not consider this effect any further. There was also a clear effect of *Laterality*, $F(1,17) = 20.16$, $p < .001$, indicating a more negative ERP contralateral to the side of the target face.

One effect differed markedly between the ANOVA on average ERPs and the whole-scalp BF analysis: The ANOVA showed a highly significant *Preview × Laterality* interaction, $F(1,17) = 21.53$, $p < .001$, though a low BF = 0.33 emerged from Bayesian analysis of the same values (see also Fig. 6E). This discrepancy between frequentist and Bayesian results suggests that the effect is not reliable, although it would have been theoretically meaningful. The direction of the interaction suggested a larger preview effect – expressed in the difference between valid and invalid trials – at electrodes contralateral versus ipsilateral to target/saccade direction. Though the target was foveated, any preview-face-related activity was possibly lateralized, since the preview face was presented in the periphery and, therefore, projected primarily to the contralateral hemisphere. Pre-saccadic preview-related activity might have remained to some degree lateralized across the saccade, and therefore it is plausible that also the preview effect was larger in the hemisphere contralateral to saccade/cue direction.

The ANOVA at electrode CPz on average amplitudes for the 320–400 ms time window confirmed the *Preview × Target Orientation* interaction, $F(1,17) = 10.68$, $p = .005$, and corroborated the more pronounced target face inversion effect (upright minus inverted) with an invalid ($-1.19\,\mu V$) compared to with a valid ($-0.07\,\mu V$) preview. This ANOVA also showed a main effect of *Target Orientation*, $F(1,18) = 5.90$, $p = .027$. No other effects were statistically significant.

3.4. Experiment 2 replicates the effects from experiment 1 in tilt discrimination performance and in the FRP

In contrast to Experiment 1, Experiment 2 contained a more restrictive selection of face stimuli, which were only presented to the left of fixation, and the proportion of valid and invalid trials was manipulated to

achieve a mostly-valid (66.6% valid, 33.3% invalid) block and a mostly-invalid (33.3% valid, 66.6% invalid) block. Overall, Experiment 2 replicated the preview effects in both behavior (Fig. 7) and FRP data (Fig. 8). Response times in the tilt discrimination task were faster in valid than in invalid preview conditions, $F(1,18) = 31.58$, $p < .001$, BF = 4.89 (Fig. 7A). There was no preview effect in error rates $F(1,18) < 1$, BF = 0.19 (Fig. 7B). The FRP again exhibited a pronounced preview effect in the fN170 component (Fig. 8E), which was corroborated by a repeated measures ANOVA on average ERPs at right hemisphere electrode PO8 in the time window 165–250 ms, $F(1,22) = 41.46$, $p < .001$. Note that, since preview face stimuli were only presented in the left visual field in this experiment, we focused the ERP analysis on the right hemisphere (i.e. electrode PO8). The evidence for the preview effect was, however, similar at the corresponding electrodes on the left hemisphere, as can be seen in Fig. 8E.

Like the preview effect, also the clear target orientation effect from Experiment 1 was replicated in Experiment 2. Responses in the tilt discrimination task were faster, $F(1,18) = 14.23$, $p = .001$, BF = 10.00, and clearly more accurate, $F(1,18) = 36.94$, $p < .001$, BF > 100, for upright than inverted target faces. Furthermore, the FRP showed again a clear target face inversion effect from about 150 ms onwards that further extended across the whole post-fixation period. Importantly, the target orientation effect was present in the fN170 component consisting in a more negative deflection for inverted compared to upright target faces (BF evidence in Fig. 9A, ERPs in Fig. 9E). This effect was confirmed by an ANOVA at PO8, time window 165–250 ms, with $F(1,18) = 14.54$, $p = .001$.

Additionally, error rates indicated an interaction of *Preview* and *Target Orientation* factors, $F(1,18) = 7.00$, $p = .016$, which can be interpreted as a *Preview Orientation* main effect. This effect indicated slightly higher error rate with inverted (21.8%) compared to upright (20.5%) preview faces. The BF for this effect was, however, indecisive and, if anything, suggested the absence an effect, BF = 0.47. We do not further consider this effect.

As in Experiment 1, the early FRP also showed a clear *Preview × Target Orientation* interaction – the statistical expression of a *Preview Orientation* effect – starting already at around 50 ms and extending to 170 ms post fixation onset (Fig. 9C). As can be seen from Fig. 9E, this effect reflected a more negative P1 with inverted compared to upright preview faces, although the preview face was replaced by the target face at that point of the trial and the target face could have had a different overall orientation.

Again, as in Experiment 1, evidence for the *Preview × Target Orientation* interaction became positive again around 350 ms over central-parietal cortex (Fig. 9C). When evaluated at electrodes CPz in the time window 320–400 ms, the target orientation effect - consisting of a stronger negativity for inverted compared to upright targets, $F(1,18) = 5.59$, $p = .030$ - was more pronounced with an invalid ($-1.20\,\mu V$) rather than valid preview ($0.13\,\mu V$), $F(1,18) = 11.49$, $p = .003$. As in Experiment 1, this likely reflects increased processing of the target face orientation if the target presents information that conflicts with the preview. Overall, the results of Experiment 2 reproduced the results observed in Experiment 1.

3.5. Experiment 2: The proportion manipulation affected tilt discrimination performance and the FRP, but it did not modulate the magnitude of the preview effect in the fN170

Experiment 2 tested whether the preview effect found in Experiment 1 was the result of a contextual prediction mechanism across trials, in the sense that it is influenced by expectations based on the frequency of events over an extended period of time rather than a single saccade. If the preview effect results from such a context-specific prediction mechanism, then it should be larger in blocks with mostly valid trials compared to blocks with mostly invalid trials (Fig. 3). We therefore expected to find a *Preview × Proportion* interaction in the behavioral data of the tilt discrimination task and in the N170 component of the FRP.
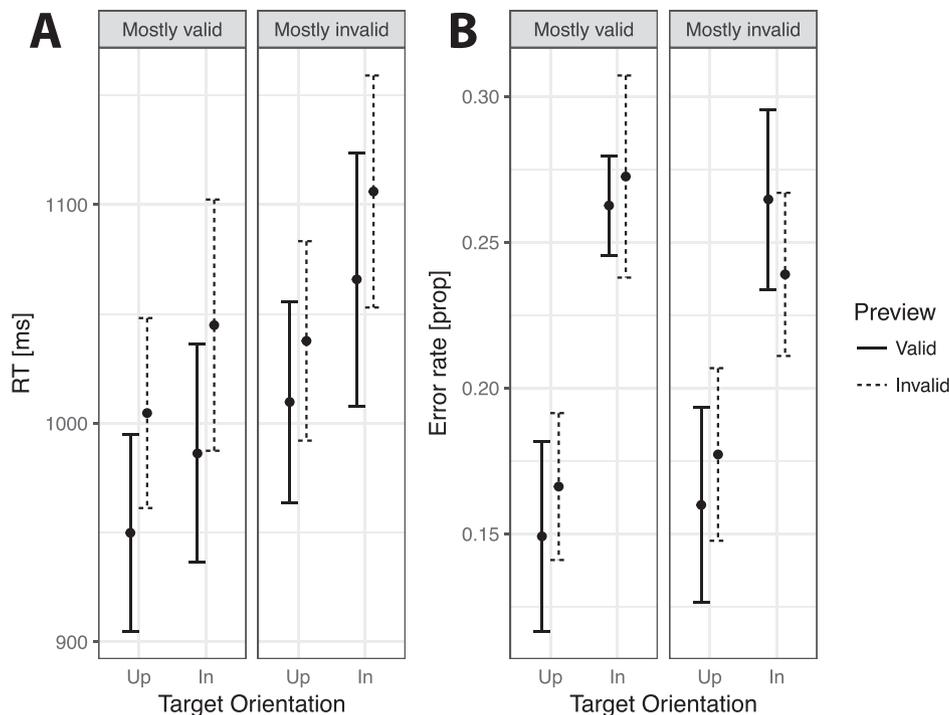
Fig. 7. Behavioral results of Experiment 2. Response times (panel A) were faster in valid than in invalid trials, and faster for upright (Up) than for inverted (In) targets. The evidence for the Preview (valid, invalid) by *Proportion* (mostly valid, mostly invalid) interaction was unclear (see text). Error rate (panel B) was lower for upright than for inverted targets.

Interestingly, some hint for a *Preview × Proportion* interaction was provided by response times, $F(1,18) = 5.64$, $p = .029$, suggesting a slightly larger preview effect (57 ms) in the mostly valid block compared to the mostly invalid block (34 ms), which was the expected direction of the effect. However, the corresponding BF = 0.29 suggested no effect of this interaction, which renders the evidence rather uncertain. Another inconsistency in the response time data manifested in the main effect of *Proportion* which was not significant, $F(1,18) = 2.14$, $p = .161$, but exhibited BF = 38.23.

In the error rates, the *Preview × Proportion* interaction was not significant, $F(1,18) < 1$ (absence of effect confirmed by BF = 0.33) and also the *Proportion* main effect was not significant, $F(1,18) = 0.05$, $p = .828$ (absence of effect confirmed by BF = 0.18).

In contrast to these equivocal behavioral results, the EEG data provided compelling evidence for the same fN170 preview effect in both mostly-valid and mostly-invalid blocks. BF values less than 0.33 at posterior lateral electrodes, where the fN170 preview effect is located, indicated the clear absence of a *Preview × Proportion* interaction (Fig. 8F), and this was supported in repeated measures ANOVA analysis on ERPs at PO8 from 165 to 250 ms, $F(1,18) = 0.32$, $p = .581$, at PO7, $F(1,18) = 0.57$, $p = .462$. As can be seen from the ERPs in Fig. 8G, the difference in the amplitude between valid (solid line) and invalid trials (dashed line) was the same in mostly-valid and in mostly-invalid blocks. This crucial result suggests that the magnitude of the trans-saccadic preview effect in the fN170 component is not the result of context-sensitive predictions, which contrasts ideas about the predictive nature of the N170 (Johnston et al., 2017).

One might argue that the proportion manipulation was simply not strong enough to trigger a change in the fN170 preview effect. The proportion manipulation had, however, a pronounced influence on the FRP, in particular contralateral to the target face (right hemisphere) at posterior electrodes (Fig. 9B). The direction of this effect at electrode PO8 is illustrated in Fig. 8G, with a more negative fN170 component emerging in the mostly-valid rather than mostly-invalid condition. This effect emerged in an ANOVA on ERPs at PO8, time window 165–250 ms,

$F(1,18) = 12.77$, $p = .002$. This clear influence of the proportion manipulation demonstrates that the 66.6% versus 33.3% manipulation was strong enough to influence neural processing. This effect in the EEG was probably linked to a difference in gaze behavior. As demonstrated in the analysis of gaze behavior (section 3.8. above), there was also a difference in gaze behavior between the two blocks: a proportion main effect emerged in the distribution of fixations on the target face. This pattern of results suggest that the proportion manipulation was indeed strong enough to affect the participants' gaze behavior and their EEG response, although it did not modulate the magnitude of the preview effect in the fN170.

Apart from these *Proportion* effects of main interest, the factor *Proportion* interacted with *Target Orientation* later in the FRP and, surprisingly, in ipsilateral electrodes (Fig. 9D and G). The effect was significant in an ANOVA on average ERPs at PO7, time window 550–800 ms, $F(1,18) = 6.34$, $p = .021$, suggesting that the late target face orientation effect was larger in the mostly valid than in the mostly invalid block. This effect possibly indicates some variation in higher-level processing of the target face depending on the long-run frequency of valid and invalid trials. The reasons for its direction and for its ipsilateral location are, however, unclear. In any case, this finding does not influence our conclusions about the preview effect and its modulation by proportion.

3.6. Experiment 2: Evidence for pre-saccadic expectations in the preview-locked EEG response

If the proportion manipulation consisting in a block of mostly valid and a block of mostly invalid trials introduced expectations about the validity of a single trial, the preview face might have already been processed differently in mostly valid compared to mostly invalid blocks. Thus, expectation or prediction effects might already be present before the eye-movement during the preview period. We therefore analyzed the pre-saccadic period of the EEG signal, time-locked to the preview face display onset, with the factors *Preview Orientation* (upright, inverted), *Proportion* (mostly valid, mostly invalid), and *Target Orientation* (valid,
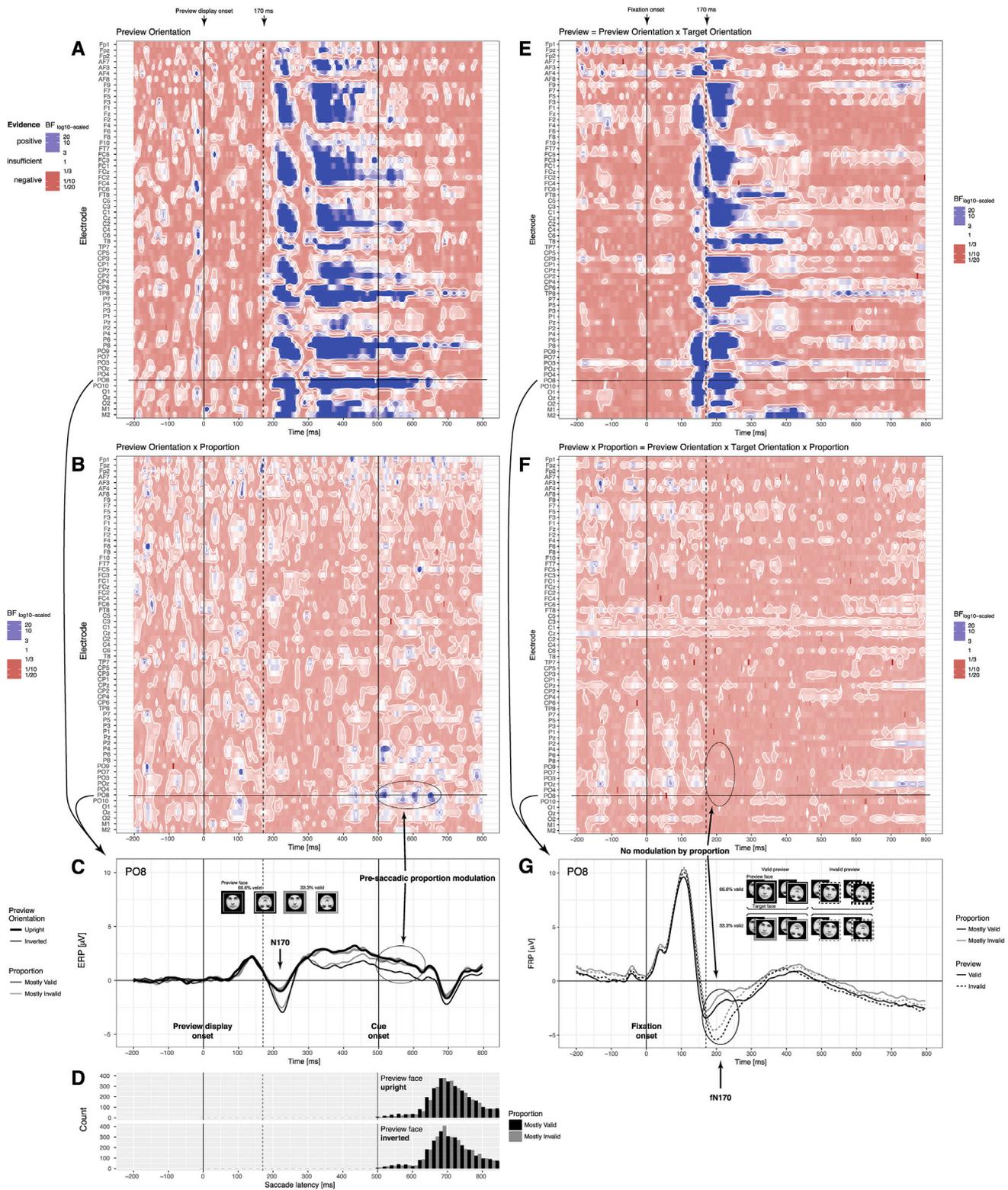
Fig. 8. Whole-scalp Bayes factor, ERPs, FRPs, and saccade latencies of the most important effects of Experiment 2 time-locked to preview display onset (ERP, panels A–D) and time-locked to fixation onset (FRP, panels E–G). The preview period (panel A) showed positive evidence for a *Preview Orientation* effect in the N170 and in a later component from ca. 300 ms. Both effects showed more negative deflections for inverted than for upright preview faces (panel C). With cue onset and before onset of most of the saccades (pane D) this face inversion effect at posterior lateral electrodes disappeared earlier in the mostly invalid than in the mostly valid block (panel C), evidenced by a *Preview Orientation × Proportion* interaction (panel B). The preview effect in the fN170 established in Experiment 1 was replicated in Experiment 2 (panel E). Crucially, the fN170 preview effect was the same in mostly valid and mostly invalid blocks (panel G) as evidenced by a BF clearly lower than 1/3 for the *Preview × Proportion* interaction (panel F). Note that panel G contains ERPs averaged across both target orientations (upright, inverted). For effects of target orientation see Fig. 9. Baseline correction was conducted for the −200 to 0 ms time window before preview display onset (panel C).
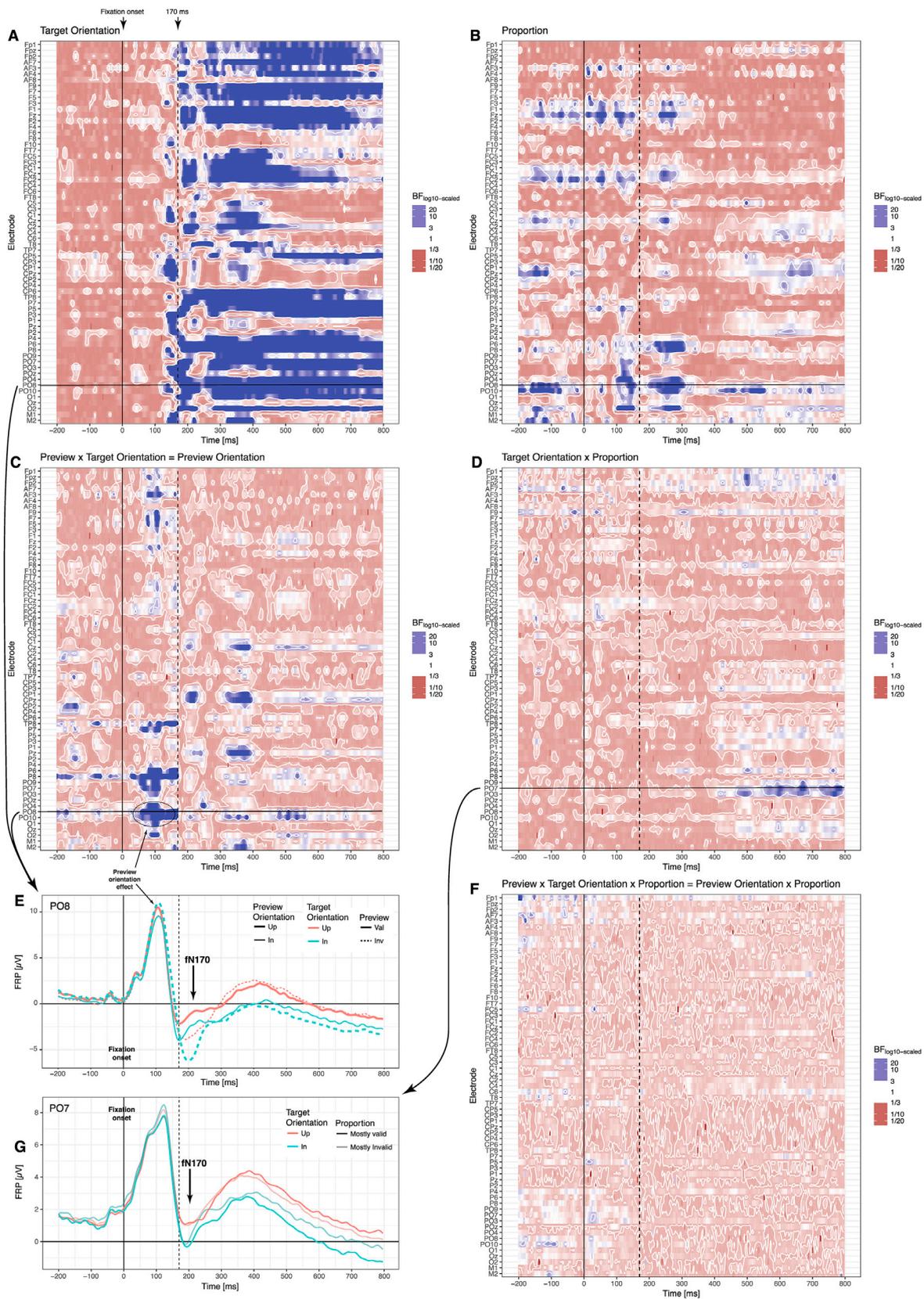
Fig. 9. Fixation-locked whole-scalp Bayes factor (BF) for the remaining main and interaction effects of Experiment 2 not illustrated in Fig. 8. The effects of Experiment 1 were replicated. *Target Orientation* elicited again a pronounced face inversion effect in the fN170 and a later component commencing at ca. 300 ms post-fixation onset (panel A, panel E). *Preview Orientation* showed again a face inversion effect in the initial phase of post-saccadic processing before 170 ms after fixation onset (panel C, panel E). In addition, the evidence for a more negative fN170 in mostly valid compared to mostly invalid blocks was clearly positive (*Proportion* main effect, panel B, corresponding ERPs in Fig. 8G). Finally, the *Target Orientation* effect was more sustained in the mostly valid compared to the mostly invalid blocks in a very late time window and surprisingly at ipsilateral sites (panel D). Evidence for the three-way interaction was largely indecisive (panel F).

invalid). It is important to note that target orientation was unknown during the preview period and that the preview face was actually task-irrelevant since the task only involved the tilt of the post-saccadic target stimulus.

First, we found a classical N170 face inversion effect in response to preview face orientation as expected from an EEG study using face stimuli. Strong evidence from a whole-scalp BF (Fig. 8A) demonstrated a more pronounced N170 for inverted compared to upright preview faces (Fig. 8C). This effect was corroborated by an ANOVA on ERPs at PO8, from 200 to 260 ms, $F(1,18) = 29.63$, $p < .001$. Compared to previous EEG studies on face perception showing an onset of the N170 largely around 150–200 ms (Bentin et al., 1996; Eimer, 2000; Eimer et al., 2010; Itier and Taylor, 2004a, 2004b; Rossion et al., 2000; Towler et al., 2012; Watanabe et al., 2003), our N170 appeared rather late at 200 ms (Fig. 8A). This discrepancy might be explained by a difference in stimulus position. Previous studies on the N170 usually presented faces at the fovea (for an exception see Pajani et al., 2017), whereas our stimuli occurred further from fixation (cf. Buonocore et al., 2019, for a similar result in this respect).

Instead of impacting early stages of post-saccadic processing, the proportion manipulation influenced later stages of the face inversion effect. Specifically, in the second half of the preview period, an inverted preview face led to a more negative deflection than an upright preview face (Fig. 8A and C), corroborated by an ANOVA on average ERPs at PO8, from 300 to 450 ms, $F(1,18) = 21.70$, $p < .001$. This effect possibly reflects a modulation of the N250 or N400 face processing components (Schweinberger and Neumann, 2015). Interestingly, as can be seen from Fig. 8C, this late preview face orientation effect declined earlier in the mostly invalid than in the mostly valid block. In particular, between cue onset (at 500 ms) and saccade onset (see the histogram of saccade latencies in Fig. 8D) the preview face orientation effect had disappeared in the mostly invalid block but was still present in the mostly valid block. This earlier reduction of the preview face orientation effect in the mostly invalid compared to the mostly valid blocks around the time of cue onset is further illustrated in the scalp maps in Fig. 10. BF evidence for the corresponding *Preview Orientation* × *Proportion* interaction is presented in Fig. 8B. An ANOVA on average ERPs at PO8, 450–600 ms post preview onset, corroborated this interaction, $F(1,18) = 16.99$, $p = .001$. Critically, this effect could not simply be explained by a difference in saccade latencies between mostly valid and mostly invalid blocks, because saccade latencies did not differ between *Preview Orientation* and *Proportion* conditions: *Proportion* main effect, $F(1,18) = 0.63$, $p = .439$, BF = 1.14, *Preview Orientation* main effect, $F(1,18) = 0.14$, $p = .714$, BF = 0.17, *Preview Orientation* × *Proportion*, $F(1,18) = 0.00$, $p = .997$, BF = 0.24. As expected, also the factor *Target Orientation* did not affect saccade latencies, all $ps > .089$, all BFs <0.29. The more sustained preview orientation effect in the mostly valid compared to the mostly invalid block might therefore reflect the degree to which the target image was processed or the degree of expectations about the upcoming target orientation based on the pre-saccadic input.

Apart from these effects of main interest, the whole-scalp analysis of the pre-saccadic period revealed also a main effect of *Proportion* (Fig. 11A), and some unsystematic effects involving *Target Orientation*

(Fig. 11B–E). The main effect of *Proportion* simply suggests a more positive ERP primarily at PO10 and at central-parietal electrodes in the mostly invalid compared to the mostly valid condition between cue onset and saccade onset, corroborated by an ANOVA on average ERPs, 500–650 ms after preview onset, at PO10, $F(1,18) = 17.54$, $p = .001$. This effect emphasizes that the influenced of *Proportion* on the EEG response in general. Compared to the other effects observed in this dataset, the effects involving *Target Orientation* were very short-lived and their spatiotemporal pattern varied considerably (Fig. 11B–E).

3.7. Experiment 2: The onset of the N170 face inversion effect in the preview period was later than the onset of the FRP N170 face inversion effect

As can be seen from Fig. 8, the N170 in the event-related potential (ERP) elicited by the onset of the preview display appeared a bit later than the N170 in the FRP (see in particular Fig. 8C–G). To determine the statistical evidence for this effect, we computed onset latencies of the face inversion effect expressed as difference waveform between trials with upright and inverted faces at electrode PO8. Specifically, we computed upright-minus-inverted preview orientation ERPs separately for mostly valid and mostly invalid blocks for the ERP aligned to the preview display. For the FRP, we computed upright-minus-inverted target orientation ERPs separately for mostly valid and mostly invalid blocks and also separately for trials with valid and invalid preview. The design for the latency onset analysis was, thus, a 2 (*Proportion*: mostly valid, mostly invalid) × 3 (*Preview*: valid/FRP, invalid/FRP, undefined/ERP) design. Onset latencies of the face inversion effect were defined via a 50% peak amplitude criterion based on jack-knifed subsamples. In other words, the onset latency was the time stamp of the sample at which the leave-one-participant-out averaged difference waves between upright-minus-inverted face ERPs reached the value closest to 50% of its maximum activation within 100–250 ms after preview-display-onset/fixation-onset (Miller et al., 1998; Ulrich and Miller, 2001). These latency onset values were subjected to a repeated measures ANOVA with the factors *Preview* (valid/FRP, invalid/FRP, undefined/ERP) and *Proportion* (mostly valid, mostly invalid). The resulting F and p-values were corrected for the reduced error introduced by jack-knifing (Ulrich and Miller, 2001). It is at present unclear how a Bayes factor would have to be corrected for the reduced error due to jack-knifing. To avoid this issue, we applied the correction factor that counteracts the reduction in error, $(n-1)^2$ (Ulrich and Miller, 2001, see in particular Appendix), to the error sum of squares term obtained from the ANOVA, which allows Bayes factor approximations (Huber-Huber, 2016; Masson, 2011; Nathoo and Masson, 2016; Wagenmakers, 2007).

This latency onset analysis of the preview-locked and the fixation-locked face inversion difference waves showed a main effect of *Preview* (valid/ERP, invalid/ERP, undefined/FRP), $F(2,36) = 27.18$, $p < .001$, $BF_{approx} > 100$. Post-hoc tests based on Scheffe's interval as critical difference (Ulrich and Miller, 2001) revealed a significantly (at alpha-level 0.05) shorter latency of the face inversion effect in the valid/FRP than in both the invalid/FRP and the undefined/ERP condition, but not between the invalid/FRP and the undefined/ERP condition (Fig. 12). Both the
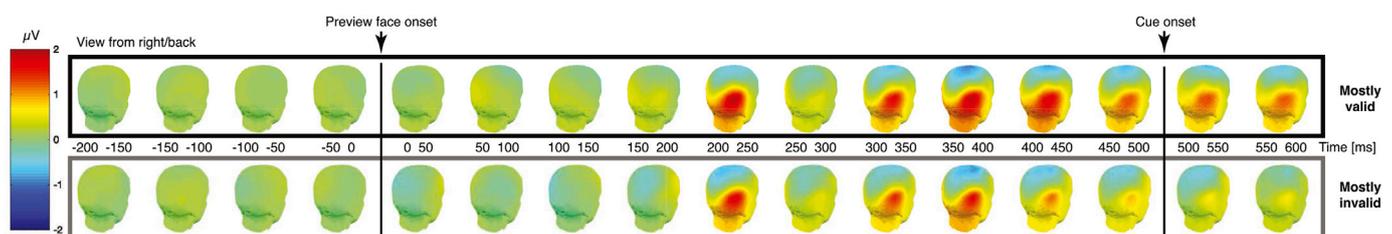

Fig. 10. Scalp map of the preview-display-onset locked face inversion effect at lateral posterior sites (upright minus inverted). In the mostly valid block (upper row) the late face inversion effect remained, whereas it declined before cue onset and disappeared with cue onset in the mostly invalid block (lower row). Evidence for the corresponding *Preview Orientation* × *Proportion* interaction in Fig. 8B.
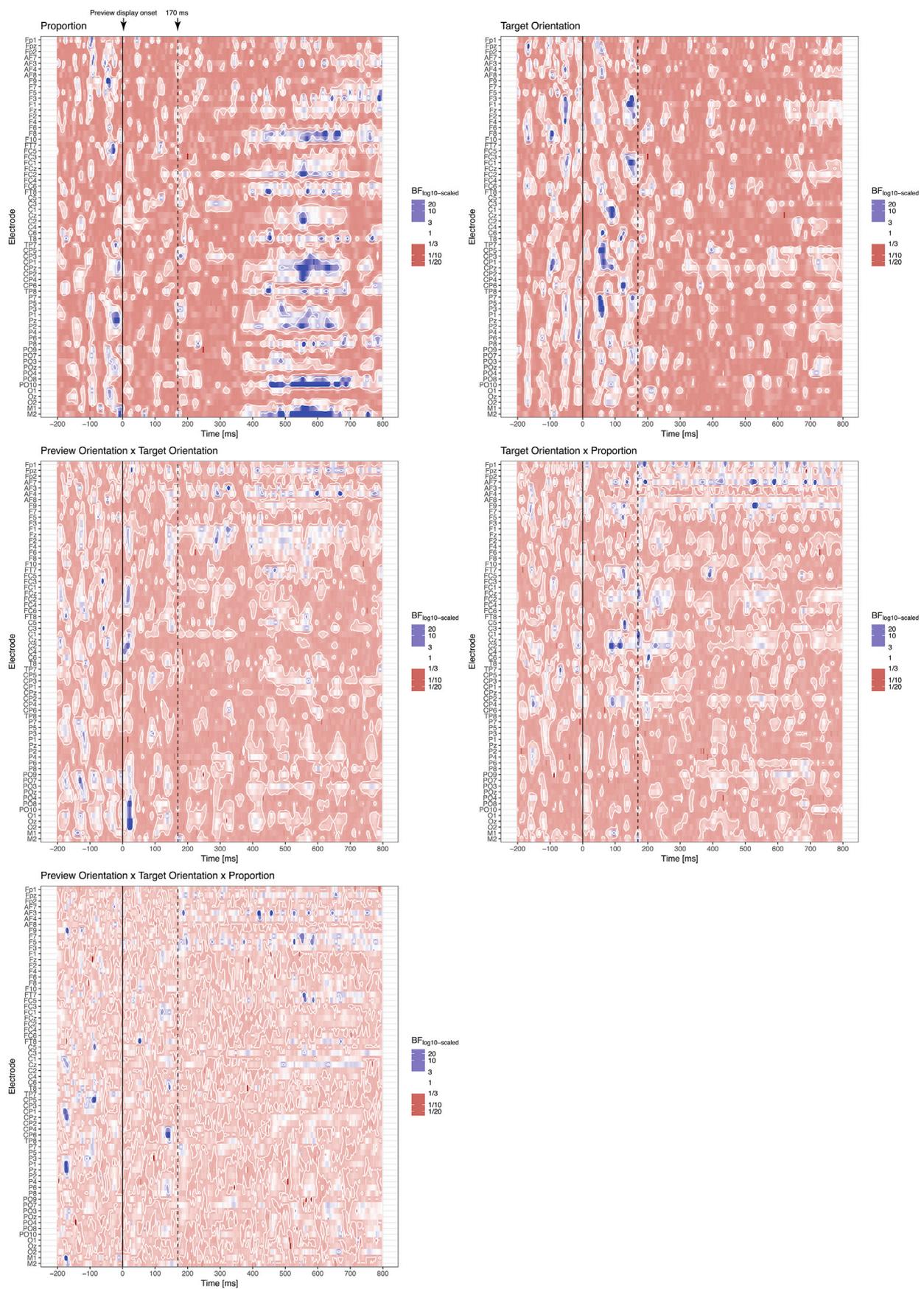
Fig. 11. Preview onset-locked whole-scalp Bayes factor (BF) for the remaining main and interaction effects of Experiment 2 not illustrated in Fig. 8. Some positive evidence for a main effect of proportion was present primarily at PO10 and some central-parietal electrodes (panel A). The other effects involving *Target Orientation* (panel B–E) showed spatio-temporally extremely limited and unsystematic patterns of occasional positive evidence.

factor *Proportion*, $F(1,18) = 0.70$, $p = .413$, $BF_{approx} = 0.330$, and the *Preview* × *Proportion* interaction, $F(2,36) = 0.15$, $p = .863$, $BF_{approx} = 0.031$, were not significant.

3.8. Experiments 1 and 2: Gaze characteristics

In order to rule out possible confounds resulting from systematic difference in gaze behavior across conditions, we analyzed saccade size, fixation duration, and the spatiotemporal distribution of target fixations in the same designs and with the same set of trials as in the corresponding behavioral and EEG data analyses.

We first checked whether the fN170 preview effect could have been confounded to some extent by *saccadic amplitudes*. The effect occurred at the time of the first post-saccadic positive deflection, which is also known as the lambda response, and this component is certainly influenced by saccade amplitude (e.g. Dimigen et al., 2011; Kaunitz et al., 2014; Ries et al., 2018). In Experiment 1, no significant effects in saccade amplitude were found; only Bayes factors provided strong evidence for a difference in saccade amplitude between saccades to the left (8.07°) and right (8.28°), $F(1,17) = 2.76$, $p = .115$, $BF > 100$. This piece of evidence might provide some weak explanation for the saccade/cue direction effect in the FRP signal (cf. Fig. 6A), however, because of the lack of any interaction effects with preview and face orientation, it cannot fully account for the fN170 preview effect and does, thus, not present a confound. Saccadic reaction times in Experiment 2 did not differ significantly across conditions and Bayes factor provided evidence for absence of all effects. Differences in saccade size across conditions cannot therefore account for the face orientation effects in the EEG.

We then checked whether differences in *fixation durations* across conditions could have affected the FRP, in particular at later stages, despite ocular artefact correction (see section 2. *Materials & Methods*). Surprisingly, in both Experiments 1 and 2, target fixation durations differed depending on the orientation of the preview face. In Experiment 1, upright preview faces led to longer subsequent target fixations (538 ms) than inverted preview faces (487 ms), $F(1,17) = 18.24$, $p = .001$, $BF = 30.54$. This effect further appeared to be modulated by *Cue Direction*, $F(1,17) = 16.19$, $p = .001$, however with a weak $BF = 1.43$, which suggested an influence of preview face orientation primarily for saccades to the right, $F(1,17) = 29.95$, $p < .001$, $BF > 100$, and not for saccade to the left, $F(1,17) = 2.40$, $p = .139$, $BF = 0.38$. The same preview orientation effect was present in Experiment 2, $F(1,18) = 7.53$, $p = .013$, $BF = 20.75$ (upright 637 ms, inverted 595 ms), which featured only saccades to the left per design and therefore contrasts Experiment 1. In addition, in Experiment 2, *Preview Orientation* interacted with *Target Orientation* presenting a *Preview* effect, $F(1,18) = 5.52$, $p = .030$, $BF = 1.50$, providing weak evidence for somewhat longer fixations with valid (629 ms) than with invalid previews (603 ms). These mixed results

demonstrate an influence of the preview face orientation on post-saccadic processing. We can, however, only speculate about the reasons for this effect. In general, inverted faces are uncommon in our everyday lives. Thus, inverted preview faces might elicit shorter primary fixations in order to more quickly gain additional information about this surprising (inverted) visual input by a secondary fixation.

Importantly, the difference in fixation durations between upright and inverted preview faces in Experiment 1 and 2 and in particular the statistically weak difference between valid and invalid trials in Experiment 2 are unlikely to have confounded the preview and face orientation effects in the FRP. The early effects (around 100 ms), the fN170 effect, and the later more central *Preview* × *Target Orientation* interaction occurred in Experiment 1 more than 100 ms before the average fixation end in the condition with the shorter fixation duration (inverted preview face, 487 ms, cf. Fig. 5), and in Experiment 2 more than 200 ms before (inverted preview face, 595 ms, cf. Fig. 9). In other words, the fixation durations were too long for artifacts from the secondary saccades to influence such early components. Given this temporal sequence, it seems more likely that the effects in the EEG were actually precursors for the differences in fixation durations, rather than the other way around.

In theory, a difference in *fixation location* might also have influenced the FRP, because differences in fixation locations imply differences in low-level visual input that affect visual ERP responses (De Lissa et al., 2014). To rule out this confound, we analyzed the distribution of target fixations with *iMap4* (Lao et al., 2017). This toolbox models fixation location and duration by creating a heat map and by fitting a linear mixed model with predictors according the experimental design to each pixel of the heat map. As suggested by Lao et al. (2017), we used a Gaussian kernel with full width at half maximum (FWHM) of 1° visual angle to smooth the pixel-resolved fixation data, thereby accounting for residual spatial uncertainty and to approximate the span of foveal input. A random intercept for participants was included in the model, but we omitted random slopes because of convergence errors. Note that omitting random slopes usually overestimates associated fixed effects (Barr et al., 2013; Matuschek et al., 2017) and should therefore be avoided. Since we were interested in ruling out potential confounds, such a less conservative approach was, however, appropriate. Further, we used bootstrapping with $n = 1000$ resamples and the default clustering approach with cluster mass. In order to compare fixation distributions for both target faces left and right in Experiment 1, we mapped the fixation locations for right side targets to the left side without mirroring them, that is, by subtracting the x-axis distance between the centers of the two target faces from the x-axis coordinates of right target face fixations.

Fig. 13 shows grand-average heat maps and significant effects for Experiments 1 and 2. Target fixations accumulated around the nose in both Experiments (Fig. 13A–B). In Experiment 1, fixation patterns differed only between saccades to the left and saccades to the right
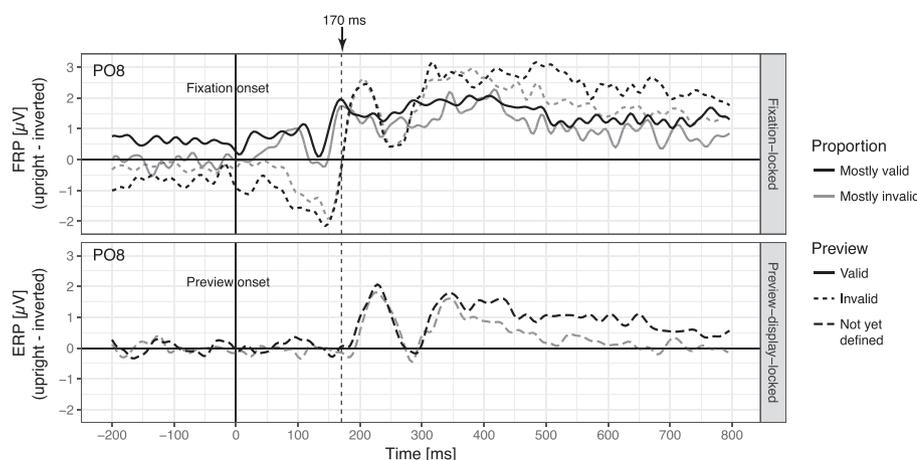

Fig. 12. Time course of the face inversion effect calculated as difference between ERPs/FRPs to upright faces minus ERPs to inverted faces separately for fixation-locked data (FRP, upper panel) and preview-display onset locked data (ERP, lower panel) averaged across both target face orientations. The onset of the face inversion effect was earliest in the post-fixation period with a valid preview peaking at 170 ms (solid lines, upper panel). In contrast, an invalid preview delayed the face inversion effect (dashed lines upper panel). The latest face inversion effect occurred in response to the preview display, that is, before any eye movement was made (lower panel). The Proportion factor did not affect face inversion effect latency.
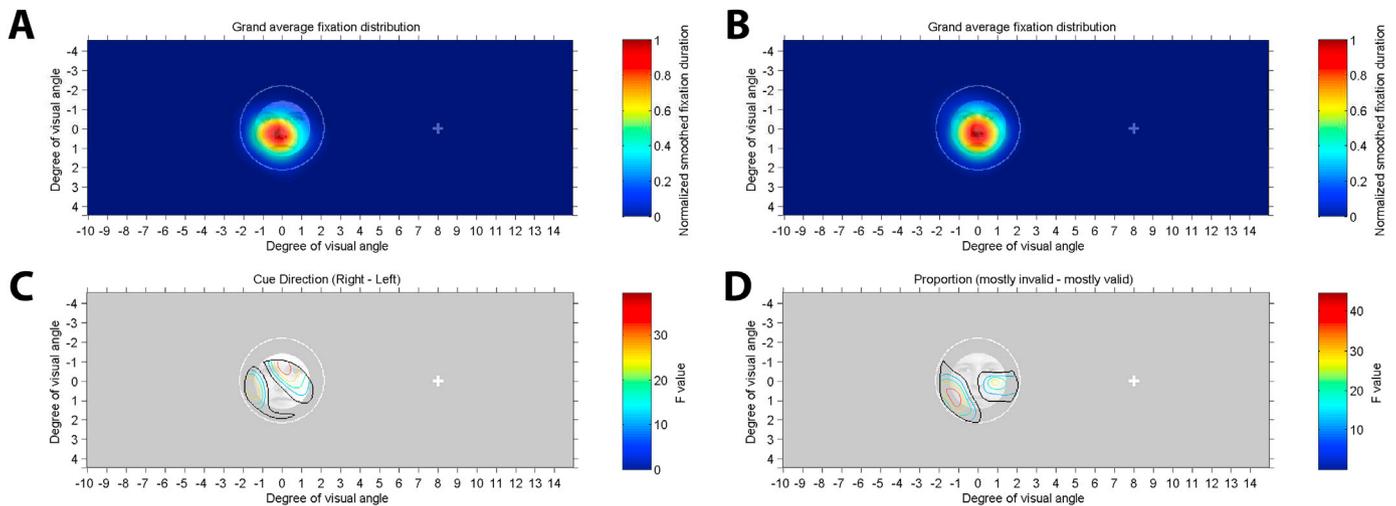
Fig. 13. Grand average fixation distribution in Experiment 1 (panel A) and 2 (panel B). Significant differences in fixations emerged in Experiment 1 only for the factor *Cue Direction* (panel C) and in Experiment 2 only for the factor Proportion (panel D). For Experiment 1, right target fixations were mapped to the left by subtracting the distance between left and right target faces from the x-axis fixation location data. The white circles around the face stimuli only illustrate the spatial threshold that determined correct target fixations during the experiment and in the analysis; they were not present in the actual display. The black contour line in panels C and D enclose areas of significant differences.

(Fig. 13C). Similar to the saccade amplitude difference mentioned above, this pattern could be related to the cue direction effects in the FRP (cf. Fig. 6A). In Experiment 2, fixation patterns differed only between the mostly valid and mostly invalid proportion blocks (Fig. 13D). This difference in gaze behavior might be related to the proportion main effect in the FRP signal (Fig. 9B). It is possible that the proportion effect in the EEG resulted from a low-level difference in visual input caused by differences in fixation distributions between blocks. This result provides further evidence that the proportion manipulation was in general strong enough to affect the participants' behavior. All other effects were not significant, which suggests that differences in the distribution of fixations on the target face cannot explain the preview and target orientation effects of main interest.

4. Discussion

We investigated the time course of trans-saccadic perception in a combined EEG and eye-tracking study. In Experiment 1, we found a peripheral preview effect both in behavior and in the lateralized posterior fN170 component. Behaviorally, participants were more efficient in discriminating target-face tilt after a valid peripheral preview than after an invalid preview. In line with this result, the fN170 component was clearly more pronounced with an invalid than with a valid preview, which is the same effect direction as the preview positivity known from reading research (Dimigen et al., 2012, in particular their Fig. 3B). Our preview effect with faces emerged, however, much earlier than the preview positivity for reading (ca. 120 ms versus ca. 180 ms post fixation). We also found a later centroparietal effect similar to the later and more central preview component in reading research (Dimigen et al., 2012, their Fig. 3B). Again, our late effect started earlier and consisted of a *Preview × Target Orientation* interaction rather than a *Preview* main effect, suggesting more in-depth processing of the target face orientation after an invalid compared to with valid preview. These results suggest that trans-saccadic integration effects can be found at different temporal scales for different types of stimuli, possibly related to the different time course for processing these stimuli at the level of categorization and meaning (e.g. Herrmann et al., 2005; Sereno and Rayner, 2003).

In addition to the trans-saccadic preview effect in the fN170, we found a clear face inversion effect (Bentin et al., 1996; Eimer, 2000; Eimer et al., 2010; Itier and Taylor, 2004a, 2004b; Rossion et al., 2000; Towler et al., 2012; Watanabe et al., 2003). This effect was also present as

expected in response times and error rates, with better performance with upright than with inverted target faces. Importantly, the target orientation and preview effects were additive, suggesting that they reflect two independent processes, one for the structural processing of faces (e.g. Bentin et al., 1996) and one for trans-saccadic integration. The additive nature of these two effects is particularly apparent when comparing the waveforms for an inverted preview face followed by an upright target face to the waveforms for an inverted preview face followed by inverted target face (Fig. 5D). These two waveforms do not differ much from each other, very likely because the preview and the face inversion effects cancelled each other out. An inverted target is expected to elicit a more negative fN170 than an upright target. Here, the inverted target was preceded by an upright preview rendering this condition invalid. The upright target was also preceded by an upright preview rendering this condition in turn valid. If both upright and inverted targets were preceded by an inverted preview face, the N170 preview effect, with a larger N170 in invalid than in valid trials, cancelled what would otherwise have appeared as a target face inversion effect.

In addition to increasing the amplitude of the fN170 in general, an invalid preview also delayed the face inversion effect. This result suggests that EEG studies in controlled experimental settings without eye movements underestimate the latency of visual EEG components during natural, unconstrained viewing situations, because real-world perception usually affords a pre-saccadic preview, resembling the valid condition here.

In Experiment 2, we asked whether the beneficial effect of the preview for post-saccadic processing, in particular on the fN170 component, was the result of a context-sensitive prediction process that takes into account validity across multiple events. In other words, does the trans-saccadic effect across a single eye movement take into account the overall frequency of valid and invalid trials? The direction of the fN170 preview effect, with a larger fN170 for invalid than for valid conditions, is consistent with a prediction error signal (Friston, 2010, 2005; Friston et al., 2012; Summerfield and Egner, 2009; see also Kornrumpf et al., 2016). If the fN170 preview effect reflected a context-sensitive predictive process, we reasoned that it should adapt to the frequency of events such that it would become larger in a block with more valid trials and smaller in a block with more invalid trials (Summerfield et al., 2008). In Experiment 2, however, the same preview effect was found in both blocks and confirmed by strong statistical evidence from a Bayes factor analysis. Our results therefore indicate that the fN170 preview effect occurs regardless

of context or recent experience, making it different from many classical prediction effects (at least in the case of 66.6% versus 33.3% valid blocks). At the same time, we do observe effects of the proportion manipulation. The N170 preview face inversion effect differed in the mostly valid compared to the mostly invalid block and there was also a corresponding difference in fixation distributions between mostly valid and mostly invalid blocks. In sum, this pattern suggests that the proportion manipulation with 33.3% versus 66.6% was strong enough to influence gaze behavior and resulting EEG correlates of face processing, but not to impact the magnitude of the post-saccadic preview effect.

Importantly, we also ruled out potentially confounding influences of saccade amplitude and fixation characteristics on the FRP results. Although we found some evidence for a relation between gaze behavior and EEG – in particular for the main effect of cue direction in Experiment 1 and the proportion main effect in Experiment 2 – differences in gaze characteristics could not explain the preview and target face orientation effects or their interactions with proportion.

The overall pattern of results provides a complex picture of how the N170 is related to visual predictions. In an elegant study, Johnston et al. (2017) showed that violating visual predictions derived from a sequences of image changes elicited an N170 even in the absence of eye movements. These authors suggested this component as a potential tool for the study of sensory predictions across saccadic eye-movements. Moreover, the source of visual prediction errors signals has been localized in the fusiform face area (de Gardelle et al., 2013a, 2013b) which has also been identified as one of the neural generators of the N170 component (e.g. Corrigan et al., 2009). Our results seem to contrast these findings.

One possibility to resolve this theoretical puzzle is that predictions across saccadic eye movements (Buonocore et al., 2019; Edwards et al., 2017; Ehinger et al., 2015) might not obey the same principles as concurrent sensory predictions in the visual system without saccades (Alink et al., 2010; Johnston et al., 2017). This conjecture implies that the N170 and the fN170 respond differently to the same type of prediction manipulation, which has not yet been tested.

An alternative is that, although all types of prediction and expectation effects are based on the regularities and statistics of the environment, there are numerous ways in which these effects can be instantiated (De Lange et al., 2018) and this might have implications for the precise neural mechanism that is targeted by the prediction manipulation. For instance, Johnston et al. (2017) studied visual prediction error signals by contrasting predictable and unpredictable image transitions within systematic sequences of images. The frequency of predictable and unpredictable trials was, however, balanced. In the present study, we manipulated the frequency of valid and invalid trials. This methodological difference may have been critical for the discrepant findings.

Finally, although proportion manipulations of 25% versus 75% have been successful in the past (Summerfield et al., 2008) and our proportion manipulation was of similar magnitude with 33.3% versus 66.6%, it might still not have been strong enough to trigger an adaptation of trans-saccadic predictions (Kovács and Vogels, 2014; Mayrhauser et al., 2014). It is well-known that effects of expectation scale with validity of the prediction just like endogenous attention scales with cue validity (Giordano et al., 2009; Kok et al., 2012). Hence, more extensive training with trans-saccadic changes than the one realized in the present design (e.g. Herwig et al., 2015; Valsecchi and Gegenfurtner, 2016) might modulate the magnitude or timing of the fN170 preview effect.

Overall, our results are consistent with the idea of three stages at which the peripheral preview might influence visual processing. First, before the saccade, the preview face inversion effect for the peripherally-presented face was more sustained in blocks with mostly valid compared to blocks with mostly invalid trials. This suggests that the preview face orientation is expected to reappear in the mostly valid block, but in the mostly invalid block participants might rather expect the opposite face orientation after the saccade. Second, at the beginning of the new fixation, we found evidence that neural activity reflected the preview rather than the image actually present at the fovea, with some interaction

between the preview and post-saccadic stimulus up to the time of the fN170. Third, at the time of the fN170, there was a preview effect consistent with the preview positivity found previously in studies with visual words but at an earlier latency than in reading. Interestingly, the trans-saccadic preview effect in the fN170 was independent of the proportion manipulation. This suggests that some aspects of trans-saccadic integration might be relatively automatic and resistant to change over the time period of one experimental session.

In any case, the preview effect in the fN170 can still be interpreted as a prediction error in terms of predictive coding (Grotheer and Kovács, 2016). In a computational sense, predictive coding only means that, instead of transmitting the complete bottom-up signal from lower to higher processing levels, only the prediction error is propagated in a feed-forward fashion (Friston, 2010; Spratling, 2017). Predictive coding therefore does not imply anything about the critical rate of occurrence of events required for adjusting top-down predictions. Thus, even though the proportion manipulation did not influence the fN170 preview effect, the preview effect itself might still have resulted from predictive coding circuits (Bastos et al., 2012), with these circuits not influenced by our proportion manipulation.

In conclusion, the current results show a strong effect of a task-irrelevant preview face on post-saccadic face processing, confirming that perception does not start anew with each new fixation. We make about three saccades every second, and it takes about 100–150 ms until visual information arrives at ventral-stream areas involved in object recognition (Foxe and Simpson, 2002). If there was no perception during that time we would miss what is going on around us for about 4 h each day (Melcher and Colby, 2008). In contrast, the *preview face* orientation effect that we found in the early stage of *post-saccadic* processing (cf. Mirpour and Bisley, 2016) suggests that, instead of waiting for new visual input after fixation onset, we perceive what was expected at that location before the eye movement began.

References

Itier, R.J., Taylor, M.J., 2004a. Source analysis of the N170 to faces and objects. Neuroreport 15, 1261–1265. https://doi.org/10.1097/01.wnr.0000127827.73576.d8.

Acunzo, D.J., MacKenzie, G., van Rossum, M.C.W., 2012. Systematic biases in early ERP and ERF components as a result of high-pass filtering. J. Neurosci. Methods 209, 212–218. https://doi.org/10.1016/j.jneumeth.2012.06.011.

Alink, A., Schwiedrzik, C.M., Kohler, A., Singer, W., Muckli, L., 2010. Stimulus predictability reduces responses in primary visual cortex. J. Neurosci. 30, 2960–2966. https://doi.org/10.1523/JNEUROSCI.3730-10.2010.

Barr, D.J., Levy, R., Scheepers, C., Tily, H.J., 2013. Random effects structure for confirmatory hypothesis testing: keep it maximal. J. Mem. Lang. 68, 255–278. https://doi.org/10.1016/j.jml.2012.11.001.

Bastos, A.M., Usrey, W.M., Adams, R.A., Mangun, G.R., Fries, P., Friston, K.J., 2012. Canonical microcircuits for predictive coding. Neuron 76, 695–711. https://doi.org/10.1016/j.neuron.2012.10.038.

Bell, A.J., Sejnowski, T.J., 1995. An information-maximization approach to blind separation and blind deconvolution. Neural Comput. 7, 1129–1159. https://doi.org/10.1162/neco.1995.7.6.1129.

Benedetto, A., Morrone, M.C., 2017. Saccadic suppression is embedded within extended oscillatory modulation of sensitivity. J. Neurosci. 37, 3661–3670. https://doi.org/10.1523/JNEUROSCI.2390-16.2016.

Bentin, S., Allison, T., Puce, A., Perez, E., McCarthy, G., 1996. Electrophysiological studies of face perception in humans. J. Cogn. Neurosci. 8, 551–565. https://doi.org/10.1162/jocn.1996.8.6.551.

Brainard, D.H., 1997. The psychophysics toolbox. Spatial Vis. 10, 433–436.

Brandman, T., Yovel, G., 2012. A face inversion effect without a face. Cognition 125, 365–372. https://doi.org/10.1016/j.cognition.2012.08.001.

Bremmer, F., Kubischik, M., Hoffmann, K.-P., Krekelberg, B., 2009. Neural dynamics of saccadic suppression. J. Neurosci. 29, 12374–12383. https://doi.org/10.1523/JNEUROSCI.2908-09.2009.

Buonocore, A., Dimigen, O., Melcher, D., 2019. Post-saccadic face processing is modulated by pre-saccadic preview: evidence from fixation-related potentials. bioRxiv 610717. https://doi.org/10.1101/610717.

Caharel, S., D'Arripe, O., Ramon, M., Jacques, C., Rossion, B., 2009. Early adaptation to repeated unfamiliar faces across viewpoint changes in the right hemisphere: evidence from the N170 ERP component. Neuropsychologia 47, 639–643. https://doi.org/10.1016/j.neuropsychologia.2008.11.016.

Castelhano, M.S., Pereira, E.J., 2017. The influence of scene context on parafoveal processing of objects. Q. J. Exp. Psychol. 1–42. https://doi.org/10.1080/17470218.2017.1310263.

Cavanaugh, J., Berman, R.A., Joiner, W.M., Wurtz, R.H., 2016. Saccadic corollary discharge underlies stable visual perception. J. Neurosci. 36, 31–42. https://doi.org/10.1523/JNEUROSCI.2054-15.2016.

Corrigan, N.M., Richards, T., Webb, S.J., Murias, M., Merkle, K., Kleinhans, N.M., Johnson, L.C., Poliakov, A., Aylward, E., Dawson, G., 2009. An investigation of the relationship between fmri and erp source localized measurements of brain activity during face processing. Brain Topogr. 22, 83–96. https://doi.org/10.1007/s10548-009-0086-5.

de Gardelle, V., Stokes, M., Johnen, V.M., Wyart, V., Summerfield, C., 2013a. Overlapping multivoxel patterns for two levels of visual expectation. Front. Hum. Neurosci. 7, 1–12. https://doi.org/10.3389/fnhum.2013.00158.

de Gardelle, V., Waszczuk, M., Egner, T., Summerfield, C., 2013b. Concurrent repetition enhancement and suppression responses in extrastriate visual cortex. Cereb. Cortex 23, 2235–2244. https://doi.org/10.1093/cercor/bhs211.

De Lange, F.P., Heilbron, M., Kok, P., 2018. How do expectations shape perception? Trends Cognit. Sci. 22, 764–779. https://doi.org/10.1016/j.tics.2018.06.002.

De Lissa, P., McArthur, G., Hawelka, S., Palermo, R., Mahajan, Y., Hutzler, F., 2014. Fixation location on upright and inverted faces modulates the N170. Neuropsychologia 57, 1–11. https://doi.org/10.1016/j.neuropsychologia.2014.02.006.

Delorme, A., Makeig, S., 2004. EEGLAB: an open source toolbox for analysis of single-trial EEG dynamics including independent component analysis. J. Neurosci. Methods 134, 9–21. https://doi.org/10.1016/j.jneumeth.2003.10.009.

Diamond, M.R., Ross, J., Morrone, M.C., 2000. Extraretinal control of saccadic suppression. J. Neurosci. 20, 3449–3455. https://doi.org/10.1038/371511a0.

Dienes, Z., 2016. How Bayes factors change scientific practice. J. Math. Psychol. 72, 78–89. https://doi.org/10.1007/s13398-014-0173-7.2.

Dimigen, O., 2018. Optimized ICA-based removal of ocular EEG artifacts from free viewing experiments. BioRxiv Prepr. https://doi.org/10.1101/446955.

Dimigen, O., Sommer, W., Hohlfeld, A., Jacobs, A.M., Kliegl, R., 2011. Coregistration of eye movements and EEG in natural reading: analyses and review. J. Exp. Psychol. Gen. 140, 552–572. https://doi.org/10.1037/a0023885.

Dimigen, O., Kliegl, R., Sommer, W., 2012. Trans-saccadic parafoveal preview benefits in fluent reading: a study with fixation-related brain potentials. Neuroimage 62, 381–393. https://doi.org/10.1016/j.neuroimage.2012.04.006.

Edwards, G., Vetter, P., McGruer, F., Petro, L.S., Muckli, L., 2017. Predictive feedback to V1 dynamically updates with sensory input. Sci. Rep. 7, 1–12. https://doi.org/10.1038/s41598-017-16093-y.

Edwards, G., VanRullen, R., Cavanagh, P., 2018. Decoding trans-saccadic memory. J. Neurosci. 38, 1114–1123. https://doi.org/10.1523/JNEUROSCI.0854-17.2017.

Ehinger, B.V., König, P., Ossandón, J.P., 2015. Predictions of visual content across eye movements and their modulation by inferred information. J. Neurosci. 35, 7403–7413. https://doi.org/10.1523/JNEUROSCI.5114-14.2015.

Eimer, M., 2000. Effects of face inversion on the structural encoding and recognition of faces. Evidence from event-related brain potentials. Cogn. Brain Res. 10, 145–158. https://doi.org/10.1016/S0926-6410(00)00038-0.

Eimer, M., Kiss, M., Nicholas, S., 2010. Response profile of the face-sensitive N170 component: a rapid adaptation study. Cereb. Cortex 20, 2442–2452. https://doi.org/10.1093/cercor/bhp312.

Ewbank, M.P., Smith, W.A.P., Hancock, E.R., Andrews, T.J., 2008. The M170 reflects a viewpoint-dependent representation for both familiar and unfamiliar faces. Cereb. Cortex 18, 364–370. https://doi.org/10.1093/cercor/bhm060.

Fabius, J.H., Fracasso, A., Van der Stigchel, S., 2016. Spatiotopic updating facilitates perception immediately after saccades. Sci. Rep. 6, 34488. https://doi.org/10.1038/srep34488.

Foxe, J., Simpson, G., 2002. Flow of activation from V1 to frontal cortex in humans. Exp. Brain Res. 142, 139–150. https://doi.org/10.1007/s00221-001-0906-7.

Frässle, S., Paulus, F.M., Krach, S., Schweinberger, S.R., Stephan, K.E., Jansen, A., 2016. Mechanisms of hemispheric lateralization: asymmetric interhemispheric recruitment in the face perception network. Neuroimage 124, 977–988. https://doi.org/10.1016/j.neuroimage.2015.09.055.

Friston, K., 2005. A theory of cortical responses. Philos. Trans. R. Soc. Lond. Ser. B Biol. Sci. 360, 815–836. https://doi.org/10.1098/rstb.2005.1622.

Friston, K., 2010. The free-energy principle: a unified brain theory? Nat. Rev. Neurosci. 11, 127–138. https://doi.org/10.1038/nrn2787.

Friston, K., Kiebel, S., 2009. Predictive coding under the free-energy principle. Philos. Trans. R. Soc. Lond. Ser. B Biol. Sci. 364, 1211–1221. https://doi.org/10.1098/rstb.2008.0300.

Friston, K., Adams, R.A., Perrinet, L., Breakspear, M., 2012. Perceptions as hypotheses: saccades as experiments. Front. Psychol. 3, 1–20. https://doi.org/10.3389/fpsyg.2012.00151.

Ganmor, E., Landy, M.S., Simoncelli, E.P., 2015. Near-optimal integration of orientation information across saccades. J. Vis. 15, 8. https://doi.org/10.1167/15.16.8.

Giordano, A.M., McElree, B., Carrasco, M., 2009. On the automaticity and flexibility of covert attention: a speed-accuracy trade-off analysis. J. Vis. 9, 1–10. https://doi.org/10.1167/9.3.30.

Grotheer, M., Kovács, G., 2016. Can predictive coding explain repetition suppression? Cortex 80, 113–124. https://doi.org/10.1016/j.cortex.2015.11.027.

Grotheer, M., Hermann, P., Vidnyánszky, Z., Kovács, G., 2014. Repetition probability effects for inverted faces. Neuroimage 102, 416–423. https://doi.org/10.1016/j.neuroimage.2014.08.006.

Helmholtz, H. von, 1867. Handbuch der physiologischen Optik [Handbook of physiological optics]. Voss, Leipzig.

Herrmann, M.J., Ehlis, A.-C., Muehlberger, A., Fallgatter, A.J., 2005. Source localization of early stages of face processing. Brain Topogr. 18, 77–85. https://doi.org/10.1007/s10548-005-0277-7.

Herwig, A., 2015. Transsaccadic integration and perceptual continuity. J. Vis. 15, 7. https://doi.org/10.1167/15.16.7.

Herwig, A., Weiß, K., Schneider, W.X., 2015. When circles become triangular: how transsaccadic predictions shape the perception of shape. Ann. N. Y. Acad. Sci. 1339, 97–105. https://doi.org/10.1111/nyas.12672.

Hinojosa, J.A., Mercado, F., Carretié, L., 2015. N170 sensitivity to facial expression: a meta-analysis. Neurosci. Biobehav. Rev. 55, 498–509. https://doi.org/10.1016/j.neubiorev.2015.06.002.

Huber-Huber, C., 2016. BIC approximation for ANOVA designs [WWW Document]. https://chsquare.shinyapps.io/BICapproxApp/.

Huber-Huber, C., Ditye, T., Marchante Fernández, M., Ansorge, U., 2016. Using temporally aligned event-related potentials for the investigation of attention shifts prior to and during saccades. Neuropsychologia 92, 129–141. https://doi.org/10.1016/j.neuropsychologia.2016.03.035.

Itier, R.J., Taylor, M.J., 2004b. Effects of repetition learning on upright, inverted and contrast-reversed face processing using ERPs. Neuroimage 21, 1518–1532. https://doi.org/10.1016/j.neuroimage.2003.12.016.

JASP Team, 2018. JASP ([Computer software]), Version 0.9.

Johnston, P., Robinson, J., Kokkinakis, A., Ridgeway, S., Simpson, M., Johnson, S., Kaufman, J., Young, A.W., 2017. Temporal and spatial localization of prediction-error signals in the visual brain. Biol. Psychol. 125, 45–57. https://doi.org/10.1016/j.biopsycho.2017.02.004.

Kaunitz, L.N., Kamienkowski, J.E., Varatharajah, A., Sigman, M., Quiroga, R.Q., Ison, M.J., 2014. Looking for a face in the crowd: fixation-related potentials in an eye-movement visual search task. Neuroimage 89, 297–305. https://doi.org/10.1016/j.neuroimage.2013.12.006.

Kok, P., Rahnev, D., Jehee, J.F.M., Lau, H.C., De Lange, F.P., 2012. Attention reverses the effect of prediction in silencing sensory signals. Cereb. Cortex 22, 2197–2206. https://doi.org/10.1093/cercor/bhr310.

Kornrumpf, B., Niefind, F., Sommer, W., Dimigen, O., 2016. Neural correlates of word recognition: a systematic comparison of natural reading and rapid serial visual presentation. J. Cogn. Neurosci. 28, 1374–1391. https://doi.org/10.1162/jocn.

Kovács, G., Vogels, R., 2014. When does repetition suppression depend on repetition probability? Front. Hum. Neurosci. 8, 1–3. https://doi.org/10.3389/fnhum.2014.00685.

Kovács, G., Iffland, L., Vidnyánszky, Z., Greenlee, M.W., 2012. Stimulus repetition probability effects on repetition suppression are position invariant for faces. Neuroimage 60, 2128–2135. https://doi.org/10.1016/j.neuroimage.2012.02.038.

Kovalenko, L.Y., Busch, N.A., 2016. Probing the dynamics of perisaccadic vision with EEG. Neuropsychologia 85, 337–348. https://doi.org/10.1016/j.neuropsychologia.2015.12.012.

Lao, J., Miellet, S., Pernet, C., Sokhn, N., Caldara, R., 2017. iMap4: an open source toolbox for the statistical fixation mapping of eye movement data with linear mixed modeling. Behav. Res. Methods 49, 559–575. https://doi.org/10.3758/s13428-016-0737-x.

Leys, C., Ley, C., Klein, O., Bernard, P., Licata, L., 2013. Detecting outliers: do not use standard deviation around the mean, use absolute deviation around the median. J. Exp. Soc. Psychol. 49, 764–766. https://doi.org/10.1016/j.jesp.2013.03.013.

Luck, S.J., Gaspelin, N., 2017. How to get statistically significant effects in any ERP experiment (and why you shouldn't). Psychophysiology 54, 146–157. https://doi.org/10.1111/psyp.12639.

Makeig, S., Bell, A.J., Jung, T.-P., Sejnowski, T.J., 1996. Independent component analysis of electroencephalographic data. Adv. Neural Inf. Process. Syst. 8, 145–151. https://doi.org/10.1109/ICOSP.2002.1180091.

Masson, M.E.J., 2011. A tutorial on a practical Bayesian alternative to null-hypothesis significance testing. Behav. Res. Methods 43, 679–690. https://doi.org/10.3758/s13428-010-0049-5.

Matuschek, H., Kliegl, R., Vasishth, S., Baayen, H., Bates, D., 2017. Balancing Type I error and power in linear mixed models. J. Mem. Lang. 94, 305–315. https://doi.org/10.1016/j.jml.2017.01.001.

Mayrhauser, L., Bergmann, J., Crone, J., Kronbichler, M., 2014. Neural repetition suppression: evidence for perceptual expectation in object-selective regions. Front. Hum. Neurosci. 8, 1–8. https://doi.org/10.3389/fnhum.2014.00225.

Melcher, D., 2011. Visual stability. Philos. Trans. R. Soc. Lond. Ser. B Biol. Sci. 366, 468–475. https://doi.org/10.1098/rstb.2010.0277.

Melcher, D., Colby, C.L., 2008. Trans-saccadic perception. Trends Cognit. Sci. 12, 466–473. https://doi.org/10.1016/j.tics.2008.09.003.

Melcher, D., Morrone, M.C., 2015. Nonretinotopic visual processing in the brain. Vis. Neurosci. 32. https://doi.org/10.1017/S095252381500019X.

Miller, J., Patterson, T., Ulrich, R., 1998. Jackknife-based method for measuring LRP onset latency differences. Psychophysiology 35, 99–115. https://doi.org/10.1111/1469-8986.3510099.

Mirpour, K., Bisley, J.W., 2016. Remapping, spatial stability, and temporal continuity: from the pre-saccadic to postsaccadic representation of visual space in LIP. Cerebr. Cortex 26, 3183–3195. https://doi.org/10.1093/cercor/bhv153.

Näätänen, R., Kreegipuu, K., 2011. The mismatch negativity (MMN). In: Kappenman, E.S., Luck, S.J. (Eds.), Oxford Handbook of Event-Related Potential Components. Oxford University Press, Oxford, New York. https://doi.org/10.1093/oxfordhb/978 0195374148.013.0081.

Nathoo, F.S., Masson, M.E.J., 2016. Bayesian alternatives to null-hypothesis significance testing for repeated-measures designs. J. Math. Psychol. 72, 144–157. https://doi.org/10.1016/j.jmp.2015.03.003.

Niefind, F., Dimigen, O., 2016. Dissociating parafoveal preview benefit and parafovea-on-fovea effects during reading: a combined eye tracking and EEG study. Psychophysiology 53, 1784–1798.

Pajani, A., Kouider, S., Roux, P., de Gardelle, V., 2017. Unsuppressible repetition suppression and exemplar-specific expectation suppression in the fusiform face area. Sci. Rep. 7, 160. https://doi.org/10.1038/s41598-017-00243-3.

Pelli, D.G., 1997. The VideoToolbox software for visual psychophysics: transforming numbers into movies. Spatial Vis. 10, 437–442.

Pisella, L., Alahyane, N., Blangero, A., Thery, F., Blanc, S., Pelisson, D., 2011. Right-hemispheric dominance for visual remapping in humans. Philos. Trans. R. Soc. Lond. Ser. B Biol. Sci. 366, 572–585. https://doi.org/10.1098/rstb.2010.0258.

Plöchl, M., Ossandón, J.P., König, P., 2012. Combining EEG and eye tracking: identification, characterization, and correction of eye movement artifacts in electroencephalographic data. Front. Hum. Neurosci. 6, 278. https://doi.org/10.3389/fnhum.2012.00278.

Polich, J., 2011. Neuropsychology of P300, the Oxford Handbook of Event-Related Potential Components. Oxford University Press, Oxford, New York. https://doi.org/10.1093/oxfordhb/9780195374148.013.0089.

Prime, S.L., Vesia, M., Crawford, J.D., 2011. Cortical mechanisms for trans-saccadic memory and integration of multiple object features. Philos. Trans. R. Soc. Lond. Ser. B Biol. Sci. 366, 540–553. https://doi.org/10.1098/rstb.2010.0184.

R Core Team, 2013. R: A Language and Environment for Statistical Computing ([software]), version 3.2.1.

Raftery, A.E., 1995. Bayesian model selection in social research. Socio. Methodol. 25, 111–163. https://doi.org/10.2307/271063.

Rayner, K., 1975. The perceptual span and peripheral cues in reading. Cogn. Psychol. 7, 65–81. https://doi.org/10.1016/0010-0285(75)90005-5.

Ries, A.J., Slayback, D., Touryan, J., 2018. The fixation-related lambda response: effects of saccade magnitude, spatial frequency, and ocular artifact removal. Int. J. Psychophysiol. 134, 1–8. https://doi.org/10.1016/j.ijpsycho.2018.09.004.

Rossion, B., Gauthier, I., Tarr, M.J., Despland, P., Bruyer, R., Linotte, S., Crommelinck, M., 2000. The N170 occipito-temporal component is delayed and enhanced to inverted faces but not to inverted objects: an electrophysiological account of face-specific processes in the human brain. Neuroreport 11, 69–74. https://doi.org/10.1097/00001756-200001170-00014.

Rossion, B., Jacques, C., 2011. The N170: Understanding the Time Course of Face Perception in the Human Brain, Oxford Handbook of Event-Related Potential Components. Oxford University Press, Oxford, New York. https://doi.org/10.1093/oxfordhb/9780195374148.013.0064.

Rouder, J.N., Speckman, P.L., Sun, D., Morey, R.D., Iverson, G., 2009. Bayesian t tests for accepting and rejecting the null hypothesis. Psychon. Bull. Rev. 16, 225–237. https://doi.org/10.3758/PBR.16.2.225.

Rouder, J.N., Morey, R.D., Verhagen, J., Swagman, A.R., Wagenmakers, E.-J., 2016. Bayesian analysis of factorial designs. Psychol. Methods 21. https://doi.org/10.1037/met0000057.

Schotter, E.R., Angele, B., Rayner, K., 2012. Parafoveal processing in reading. Attention, Perception, Atten. Percept. Psychophys. 74, 5–35. https://doi.org/10.3758/s13414-011-0219-2.

Schut, M.J., Fabius, J.H., Van der Stoep, N., Van der Stigchel, S., 2016. Object files across eye movements: previous fixations affect the latencies of corrective saccades. Atten. Percept. Psychophys. 138–153. https://doi.org/10.3758/s13414-016-1220-6.

Schweinberger, S.R., Neumann, M.F., 2015. Repetition effects in human ERPs to faces. Cortex 80, 141–153. https://doi.org/10.1016/j.cortex.2015.11.001.

Schweinberger, S.R., Huddy, V., Burton, A.M., 2004. N250r: a face-selective brain response to stimulus repetitions. Neuroreport 15, 1501–1505. https://doi.org/10.1097/01.wnr.0000131675.00319.42.

Sereno, S.C., Rayner, K., 2003. Measuring word recognition in reading: eye movements and event-related potentials. Trends Cognit. Sci. 7, 489–493. https://doi.org/10.1016/j.tics.2003.09.010.

Spratling, M.W., 2017. A review of predictive coding algorithms. Brain Cogn. 112, 92–97. https://doi.org/10.1016/j.bandc.2015.11.003.

Stefanics, G., Kremláček, J., Czigler, I., 2014. Visual mismatch negativity: a predictive coding view. Front. Hum. Neurosci. 8, 1–19. https://doi.org/10.3389/fnhum.2014.00666.

Summerfield, C., Egner, T., 2009. Expectation (and attention) in visual cognition. Trends Cognit. Sci. 13, 403–409. https://doi.org/10.1016/j.tics.2009.06.003.

Summerfield, C., Trittschuh, E.H., Monti, J.M., Mesulam, M.M., Egner, T., 2008. Neural repetition suppression reflects fulfilled perceptual expectations. Nat. Neurosci. 11, 1004–1006. https://doi.org/10.1038/nn.2163.

Summerfield, C., Wyart, V., Johnen, V.M., de Gardelle, V., 2011. Human scalp electroencephalography reveals that repetition suppression varies with expectation. Front. Hum. Neurosci. 5, 67. https://doi.org/10.3389/fnhum.2011.00067.

Towler, J., Gosling, A., Duchaine, B., Eimer, M., 2012. The face-sensitive N170 component in developmental prosopagnosia. Neuropsychologia 50, 3588–3599. https://doi.org/10.1016/j.neuropsychologia.2012.10.017.

Ulrich, R., Miller, J., 2001. Using the jackknife-based scoring method for measuring LRP onset effects in factorial designs. Psychophysiology 38, 816–827. https://doi.org/10.1111/1469-8986.3850816.

Valsecchi, M., Gegenfurtner, K.R., 2016. Dynamic re-calibration of perceived size in fovea and periphery through predictable size changes. Curr. Biol. 26, 59–63. https://doi.org/10.1016/j.cub.2015.10.067.

Wagenmakers, E.-J., 2007. A practical solution to the pervasive problems of p values. Psychon. Bull. Rev. 14, 779–804. https://doi.org/10.3758/BF03194105.

Watanabe, S., Kakigi, R., Puce, A., 2003. The spatiotemporal dynamics of the face inversion effect: a magneto- and electro-encephalographic study. Neuroscience 116, 879–895. https://doi.org/10.1016/S0306-4522(02)00752-2.

Willenbockel, V., Sadr, J., Fiset, D., Horne, G.O., Gosselin, F., Tanaka, J.W., 2010. Controlling low-level image properties: the SHINE toolbox. Behav. Res. Methods 42, 671–684. https://doi.org/10.3758/brm.42.3.671.

Winkler, I., Haufe, S., Tangermann, M., 2011. Automatic classification of artifactual ICA-components for artifact removal in EEG signals. Behav. Brain Funct. 7, 30. https://doi.org/10.1186/1744-9081-7-30.

Wolf, C., Schütz, A.C., 2015. Trans-saccadic integration of peripheral and foveal feature information is close to optimal. J. Vis. 15, 1. https://doi.org/10.1167/15.16.1.

Wurtz, R.H., 2008. Neuronal mechanisms of visual stability. Vis. Res. 48, 2070–2089. https://doi.org/10.1016/j.visres.2008.03.021.

Zimmermann, E., Weidner, R., Fink, G.R., 2017. Spatiotopic updating of visual feature information. J. Vis. 17, 1–9. https://doi.org/10.1167/17.12.6.